iScience

CellPress
OPEN ACCESS

Article

An ivermectin – atorvastatin combination impairs nuclear transport inhibiting dengue infection *in vitro* and *in vivo*

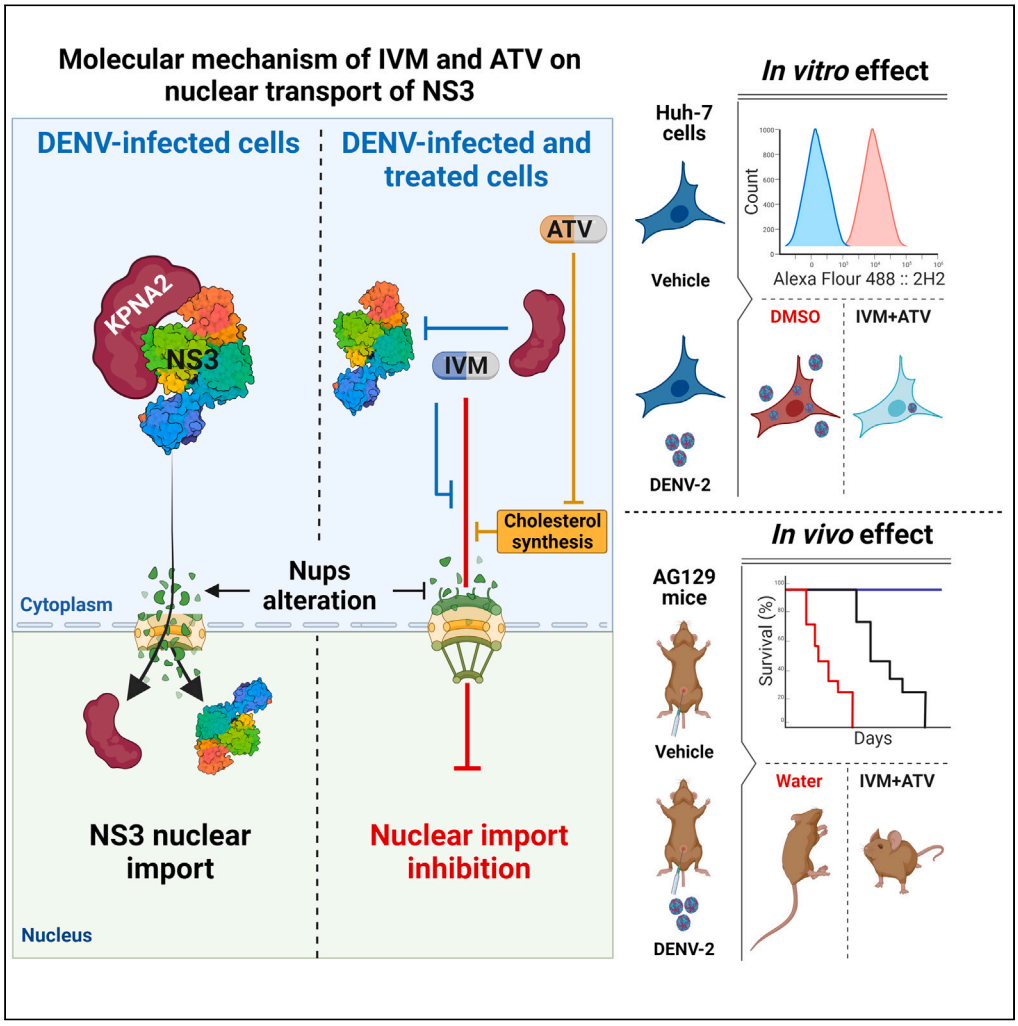

Selvin Noé Palacios-Rápalo, Carlos Noe Farfan-Morales, Carlos Daniel Cordero-Rivera, Luis Adrián De Jesús-González, José Manuel Reyes-Ruiz, Marco Antonio Meraz-Ríos, Rosa María Del Ángel

rmangel@cinvestav.mx

Highlights

The nuclear import of NS3 is blocked by ivermectin (IVM) or atorvastatin (ATV) *in vitro*

IVM+ATV combination inhibits DENV-2 infection *in vitro*

Combined IVM+ATV therapy protects AG129 mice from dengue virus disease

NS3 protein reduces its nuclear import in mice treated with an IVM+ATV combination

Palacios-Rápalo et al., iScience *26*, 108294
December 15, 2023
https://doi.org/10.1016/j.isci.2023.108294

iScience

CellPress
OPEN ACCESS

Article

An ivermectin – atorvastatin combination impairs nuclear transport inhibiting dengue infection *in vitro* and *in vivo*

Selvin Noé Palacios-Rápalo,[1] Carlos Noe Farfan-Morales,[1,2] Carlos Daniel Cordero-Rivera,[1] Luis Adrián De Jesús-González,[1,3] José Manuel Reyes-Ruiz,[4,5] Marco Antonio Meraz-Ríos,[6] and Rosa María Del Ángel[1,7,*]

SUMMARY

Dengue virus (DENV) uses cellular nuclear transport machinery to import some proteins into the nucleus. Recently, the non-structural protein 3 (NS3) of DENV was localized in the nucleus of infected cells; however, its nuclear import mechanism is still unknown. In this study, we demonstrate that Ivermectin (IVM) inhibits the nuclear localization of NS3 through the inhibition of the Importin α/β1 pathway. We also report that Atorvastatin (ATV) can modulate the nuclear transport of NS3 protease and NS5 polymerase of DENV-2. On the other hand, we found that IVM and ATV treatments reduce the alteration of nuclear pore complex (NPC) proteins, and an IVM+ATV combination reduced DENV infection both *in vitro* and *in vivo*. Hence, we conclude that ATV transport inhibition is an additional antiviral effect of this drug, suggesting a potential anti-DENV therapy in combination with IVM.

INTRODUCTION

Dengue fever is a mosquito-borne viral disease distributed worldwide in tropical and subtropical regions. It is a serious health problem due to the economic and social cost of the millions of registered annual dengue cases.[1] Unfortunately, despite the many studies on DENV, there is still no specific treatment for this disease.[2] Nonetheless, novel approaches have been explored as potential anti-DENV antivirals, such as drug repositioning that uses previously Food and Drug Administration (FDA)-approved drugs to treat other diseases.[3] Some reported anti-DENV FDA-approved drugs are lipid-lowering drugs (statins, ezetimibe), hypoglycemic drugs (metformin), and anti-parasitic drugs (Ivermectin).[4–9]

The anti-parasitic effect of IVM involves binding to ligand-gated ion channel receptors, including glutamate, Gamma-aminobutyric acid (GABA), and glycine, resulting in parasitic paralysis and death.[10] Interestingly, IVM is also a specific inhibitor of the classical nuclear import pathway, importin α/β1 (Imp α/β1), which is used by several viruses during viral replication.[11] It has been reported that RNA viruses use various mechanisms to affect cellular processes to enhance their replication and prevent the host immune response activation,[12] for example, using cellular nuclear transport proteins to import viral proteins into the nucleus.[12] Members of the *Flaviviridae* family, such as Zika virus (ZIKV), West Nile Virus (WNV), Japanese Encephalitis Virus (JEV), Hepatitis C Virus (HCV), and DENV, import viral proteins such as capsid (C), viral polymerase (NS5), and viral protease (NS3) into the nucleus during their replicative cycle using cellular nuclear transport proteins.[13–19] In this regard, the inhibition of cellular nuclear transport is currently a target for antiviral therapies.[20–22]

To be imported into the cell nucleus, cargo proteins must interact with nuclear transport proteins, commonly called importins, through a nuclear localization sequence (NLS)[23] present in the cargo protein. The cargo protein-importin complexes cross into the nucleoplasm, interacting with the nucleoporins (Nups) of the nuclear pore complex (NPC) by active transport of a Ran-Guanosine-5′-triphosphate (GTP) gradient.[23,24] It has been described that DENV NS5 polymerase is transported to the nucleus by Imp α/β1, and specific inhibition of the pathway by IVM prevents its internalization to the nucleus, affecting DENV replication.[6–8] Similar to NS5, previous research has shown that the NS3 viral protease of several members of the *Flaviviridae* family localizes in the nucleus of infected cells.[15,16,25] In particular, our research group described that the DENV-2 NS3 protein is partially localized in the nucleus of Huh7 and C6/36 mosquito-infected cells.[19,26] In addition, it has also been described that ZIKV NS3 is imported into the nucleus of Huh7 cells by Imp α/β1.[27] However, the import pathway of NS3 DENV-2 is unclear.

[1]Department of Infectomics and Molecular Pathogenesis, Center for Research and Advanced Studies (CINVESTAV-IPN), Mexico City 07360, Mexico
[2]Departamento de Ciencias Naturales, Universidad Autónoma Metropolitana (UAM), Unidad Cuajimalpa, Ciudad de México 05348, México
[3]Unidad de Investigación Biomédica de Zacatecas, Instituto Mexicano del Seguro Social, Zacatecas, Zacatecas, México
[4]Unidad Médica de Alta Especialidad, Hospital de Especialidades No. 14, Centro Médico Nacional "Adolfo Ruiz Cortines", Instituto Mexicano del Seguro Social (IMSS), Veracruz 91897, México
[5]Facultad de Medicina, Región Veracruz, Universidad Veracruzana (UV), Veracruz 91700, México
[6]Department of Molecular Biomedicine, Center for Research and Advanced Studies (CINVESTAV-IPN), Mexico City 07360, Mexico
[7]Lead contact
*Correspondence: rmangel@cinvestav.mx
https://doi.org/10.1016/j.isci.2023.108294

Nonetheless, it has been reported that during the DENV replicative cycle, the cellular cholesterol and other lipids are required,[5,28–30] and their inhibition using lipid-lowering drugs such as statins has shown anti-DENV properties.[31,32] Statins inhibit cholesterol biosynthesis by inhibiting 3-hydroxy-3-methyl-glutaryl-CoA reductase (HMGCR).[33,34] Additionally, statins impair the membrane localization of RhoGTPases, affecting intracellular signaling involved in actin cytoskeleton remodeling[35] and inhibiting cellular and viral protein transport.[36]

Interestingly, the combination of IVM and statins such as ATV reduces the nuclear accumulation of importin alpha-1 subunit (KPNA2),[37] suggesting the antiviral potential of these drugs to target importin-dependent nuclear trafficking in infections caused by Influenza virus, ZIKV, and DENV.[37] Therefore, in the present work, the effect of treatment with IVM and ATV, separately and in combination, on the nuclear transport of proteins, replication, and pathogenesis of DENV was evaluated *in vitro*. Also, we conducted an *in vivo* study to evaluate the potential effect of combined IVM+ATV therapy on the survival of DENV-2-infected AG129 mice.

RESULTS

Ivermectin inhibits importin α/β1 pathway-dependent nuclear import of Dengue virus-2 non-structural protein 3 (NS3)

Previous experiments from our group demonstrated the nuclear localization of the NS3 protein of DENV-2 at 8 h and 12 h post-infection (hpi) and in the cytoplasm at 24 hpi.[19] The nuclear localization of NS3 early after the infection of Huh7 cells with DENV-2 was confirmed by transmission immunoelectron microscopy (TIM). As expected, gold particles in the nucleus of DENV-2-infected cells were observed but not in mock-infected cells (Figure 1A) or cells incubated only with the secondary antibody coupled to 20 nm colloidal gold particles (Figure S1A). Furthermore, a higher amount of NS3 protein was detected in the nucleus of infected cells at 12 hpi compared to 24 hpi (Figures S1B and S1D), supporting our previous results.[19]

Considering the presence of NS3 in the nucleus of DENV-infected cells at 12 hpi, the effect of IVM in the NS3 location was analyzed. The toxicity of different IVM concentrations was initially evaluated (Figures S2A and S2B). The concentration of 12.5 ng of IVM was selected because of its low toxicity after incubation for 12 h. To confirm the effect of IVM, Huh7 cells were transfected with Simian Virus 40 (SV40) nuclear localization sequence (NLS) tagged to four green fluorescent proteins (SV40-x4GFP NLS). While treatment with 12.5 ng IVM during 12 h caused a significant increase in the cytoplasmic GFP fluorescence (Figure 1B), in cells treated with the vehicle dimethyl sulfoxide (DMSO), the GFP label was predominantly nuclear (Figure 1B), suggesting that 12.5 ng of IVM for 12 h can inhibit Imp α/β1-dependent nuclear transport.

Subsequently, the effect of IVM on NS3 protein localization was analyzed by confocal microscopy. Interestingly, in IVM-treated infected cells, a significant reduction in the presence of NS3 in the nucleus was observed, in contrast with DMSO-treated infected cells (Figure 1C), suggesting that NS3 protein is imported to the nucleus through Imp α/β1 pathway. Then, Huh7 cells were transfected with the wild-type NS3 protein with its cofactor NS2B (NS2B3), linked with V5-tagged in the C-terminal portion to confirm this result. Consistent with our data (Figure 1C), a significant reduction of NS3 fluorescence in the nucleus of transfected cells was observed in IVM-treated cells, compared to the transfected cells treated with DMSO (Figure 1D), confirming that NS3 protein is imported to the nucleus through the Imp α/β1 pathway (Figure 1E).

Atorvastatin blocks the nuclear transport of importin α and Dengue virus-2 NS3 protein

Given statins impair the membrane localization of RhoGTPases, affect intracellular signaling involved in actin cytoskeleton remodeling,[35] and inhibit nucleus-cytoplasmic transport,[37] the effect of ATV was evaluated on nuclear transport in DENV-infected Huh-7 cells. First, the toxicity of different ATV concentrations was evaluated (Figures S2C and S2D), and the concentration of 10 μM was selected to analyze the nuclear import inhibition, as previously reported.[37]

To initially evaluate the effect of ATV on the nuclear transport of cellular proteins, the accumulation of KPNA1 and KPNA2 in the cytoplasmic fractions of uninfected Huh7 cells treated with Vehicle, 12.5 ng IVM, or 10 μM ATV was analyzed. As fractionation purity controls, antibodies directed to Calreticulin (CRT) and Lamin A/C (LMNA) proteins were used (Figure 2A). The Western blot analysis corroborated an increase in KPNA1 and KPNA2 protein in the cytoplasmic fraction of uninfected cells during IVM and ATV treatments. However, a significant difference was only observed during ATV treatment (Figures 2B and 2C), confirming that ATV impairs the nuclear import of cellular proteins.

Based on these results, we evaluated the effect of ATV on nuclear transport in DENV-2 infected cells. As a control, uninfected cells were treated with ATV for 12 h or 24 h, and the subcellular distribution of KPNA1 was evaluated. Confocal microscopy images demonstrated a cytoplasmic increase in KPNA1 fluorescence in cells treated with ATV from 12 h (Figure 2D). Furthermore, a significant reduction of the fluorescence nucleus-cytoplasm (Fn/C) ratio at 12 h and 24 h in ATV-treated cells, compared to DMSO-treated cells, was observed (Figure 2G), confirming our Western blot assays. A similar effect was observed during SV40-x4GFP NLS transfection, where ATV treatment caused an accumulation of GFP in the cytoplasm of the cells (Figure S3C), supporting the idea that ATV inhibits karyopherin-dependent transport.

Confocal microscopy assays of DENV-2-infected cells showed that the treatment with 10 μM ATV reduced the nuclear localization of NS3 protein compared with untreated cells (Figures 2E and 2H). Likewise, ATV induced a significant reduction of the nuclear presence of NS3 in cells transfected with NS2B3 plasmid (Figure S2E), resulting in a significant decrease in the Fn/C ratio compared to DMSO-treated transfected cells (Figure S2F).

The inhibition in nuclear import induced by ATV was confirmed when the presence of NS5 protein was analyzed at 24 h post-infection.[7] A significant and robust reduction in the nuclear localization of NS5 protein was observed in ATV-treated infected cells (Figure 2F) compared to untreated cells. This result was confirmed by a decrease in the Fn/C ratio of ATV-treated compared to DMSO-treated infected cells (Figure 2I).

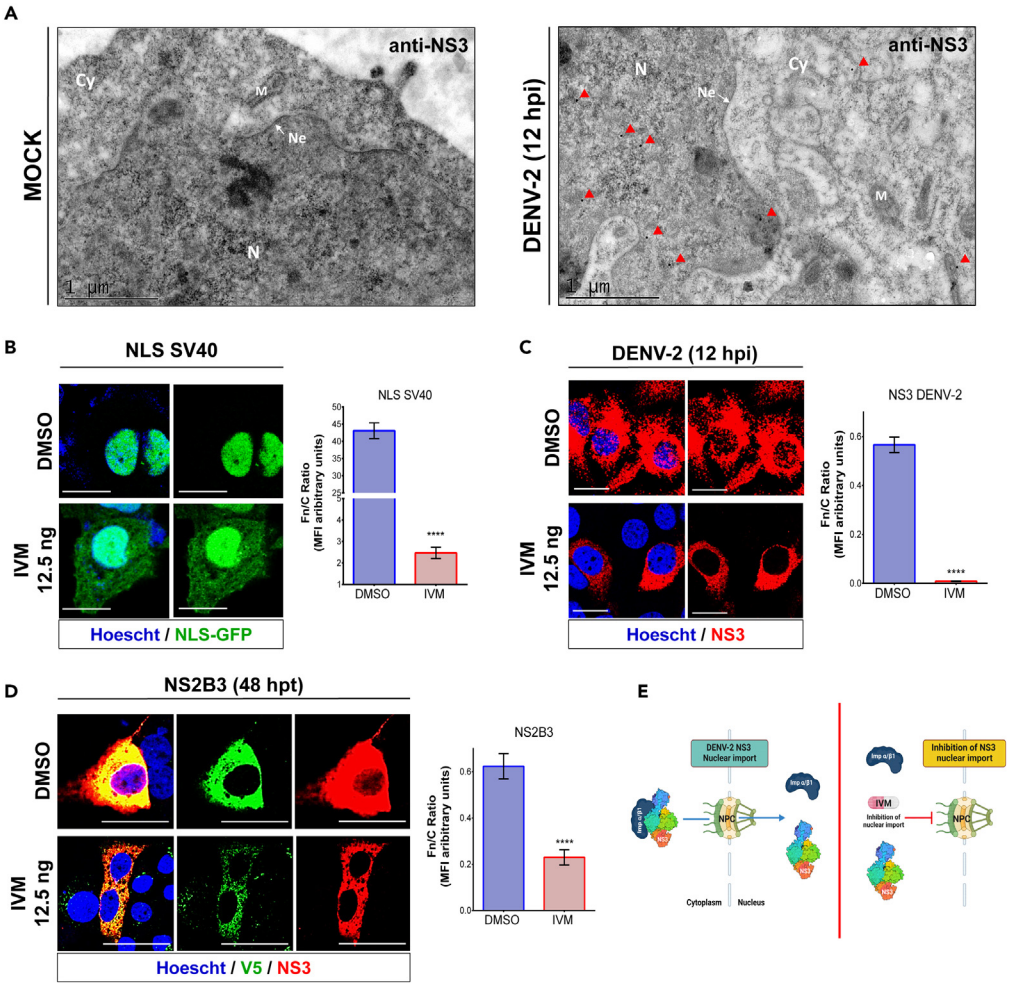

Figure 1. Ivermectin blocks the nuclear import of the NS3 protein from DENV

(A) Transmission Immunoelectron Microscopy (TIM) of Huh7 cells mock-infected or infected with DENV-2 at 12 hpi. The red arrows point to the positive colloidal gold mark for NS3. Ne: nuclear envelope, N: nucleus, Re: endoplasmic reticulum, Cy: cytoplasm, and M: mitochondria. Please see also Figure S1.

(B) Confocal microscopy images of cells transfected with SV40-x4GFP NLS, (C) infected with DENV at an MOI of 10, or (D) transfected with the plasmid encoding the NS2B3 protein of DENV in the presence of DMSO or 12.5 ng IVM. Nuclei were stained with Hoescht (blue). The first panels show merged images: scale bars, 20 µm. The GFP signal (B) and NS3 staining (C and D red) are observed in the right panel of each figure. The Mean Fluorescence Intensity (MFI) was determined for selected regions of interest (ROIs) in the nucleus and cytoplasm. The fluorescence ratio nucleus/cytoplasm (Fn/C) was determined for these selected ROIs in each confocal microscopy image (for green fluorescent protein (GFP) or NS3-Alexa-555) of cells treated or not with 12.5 ng IVM. n = 40 cells for each condition (in three independent experiments). Data were represented as mean ± standard error of the mean (SEM). Statistical comparison was performed by Two-tailed unpaired Student's t-test. ****$p < 0.0001$.

(E) Representative schematic of the mechanism of NS3 nuclear import inhibition by IVM treatment.

All these results demonstrate that ATV treatment inhibits the nuclear import of cellular proteins such as KPNA1 and KPNA2 and inhibits the nuclear transport of the NS3 and NS5 proteins in DENV-2 infected cells.

Inhibition of nuclear transport with ivermectin and atorvastatin reduces nuclear pore complex disruption during Dengue virus-2 infection

Previous studies from our group indicated that the nuclear localization of NS3 is involved in the disruption of NPC proteins.[38] If this is the case, inhibiting the nuclear import of NS3 with IVM or ATV would avoid the NPC disruption (Figures 3A and 3B). Briefly, DENV-2-infected cells were treated or not with IVM at 12.5 ng and ATV at 10 µM, and the integrity of Phenylalanine-Glycine (FG)-Nups was analyzed at 24 h using Mab414 antibody by confocal microscopy. In accordance with our previous results, the localization of NS3 was predominantly cytoplasmic at 24 hpi, with some nuclei partially stained with NS3. While the fluorescence corresponding to FG-Nups was observed as a ring structure around the nucleus of uninfected cells, this ring structure was disrupted in infected cells (Figure 3C).

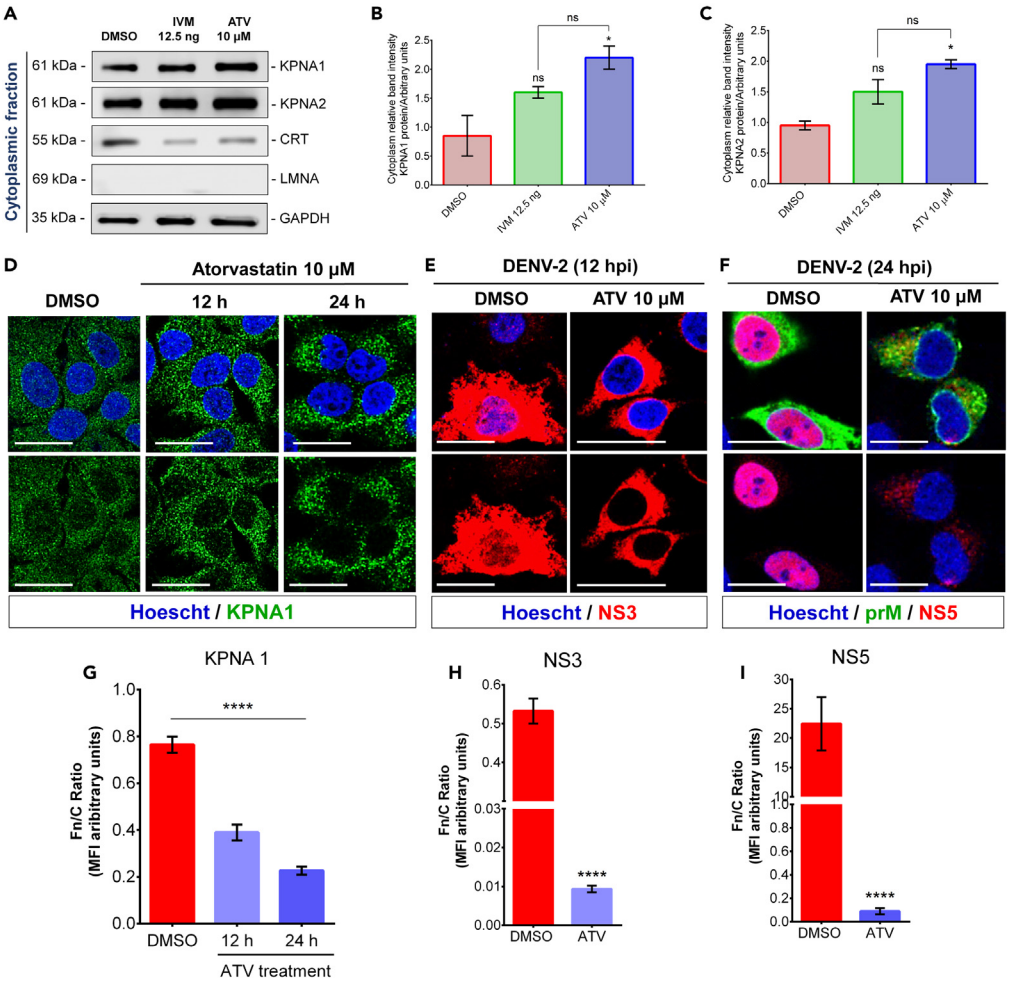

Figure 2. ATV impairs the nuclear import of NS3 and NS5 of DENV-2

(A) Western blot analysis of cytoplasmic fractions of Huh-7 cells treated with DMSO, IVM, or ATV for 24 h. Antibodies against KPNA1 and KPNA2 proteins were used. In addition, antibodies against Calreticulin (CRT) and lamin A/C (LMNA) were used as purity control of the fractions. Finally, GAPDH was used as a loading control. The graphs represent the relative intensity of (B) KPNA1 and (C) KPNA2 bands for each condition from three independent experiments. Data were represented as mean ± standard error of the mean (SEM). Statistical comparison was performed by one-way ANOVA with Tukey post-host tests. *$p < 0.05$.

(D) Confocal microscopy images of ATV treatment of uninfected or (E) infected cells at a MOI of 10 for 12 h or (F) at a MOI of 5 for 24 h. The cellular protein KPNA1 was labeled as a control for drug activity. NS3 and NS5 proteins were stained to analyze their location in ATV untreated and treated cells: scale bar, 30 µm. Please see also Figure S3C (G–I). The Mean Fluorescence Intensity (MFI) was determined for selected regions of interest (ROIs) in the nucleus and cytoplasm. The fluorescence ratio nucleus/cytoplasm (Fn/C) was determined for these selected ROIs in each confocal microscopy image (for NS3-Alexa555 or NS5-Alexa555) of cells treated or not with ATV. n = 40 cells for each condition (in three independent experiments). Data were represented as mean ± standard error of the mean (SEM). Statistical comparison was performed by Two-tailed unpaired Student's t-test. ***$p < 0.001$, ****$p < 0.0001$.

Interestingly, treatment with IVM and ATV partially prevented the disruption of FG-Nups (Figure 3C). The mean fluorescence intensity (MFI) analysis showed a significant difference between Mock and DENV-2 infected cells ($p < 0.0001$) and DENV-2 infected cells treated with IVM ($p < 0.0001$). However, the MFI of IVM-treated infected cells was significantly higher than vehicle-infected cells (Figure 3D). Similarly, ATV treatments increased the MFI of FG-Nups compared to untreated infected cells. (Figure 3D). Interestingly, we observed a smaller significant difference between Mock and ATV-treated infected cells (p 0.0035) (Figure 3D), in contrast to that observed between Mock and IVM-treated infected cells ($p < 0.0001$) (Figure 3D), suggesting that ATV has a higher protective effect against nucleoporins alteration compared to IVM (Figure 3D). All these results suggest that the presence of NS3 in the nucleus is required for NPC disruption.

The ivermectin + atorvastatin combination promotes the cytoplasmic accumulation of importin α and reduces the percentage of Dengue virus-2 infected cells

Based on our results, we aimed to evaluate the effect on nuclear transport of the two drugs in combination. For this, cell viability assays of nine different combinations of the drugs were performed at 24 h, showing that 12.5 ng IVM and 10 µM ATV in combination did not affect the cell

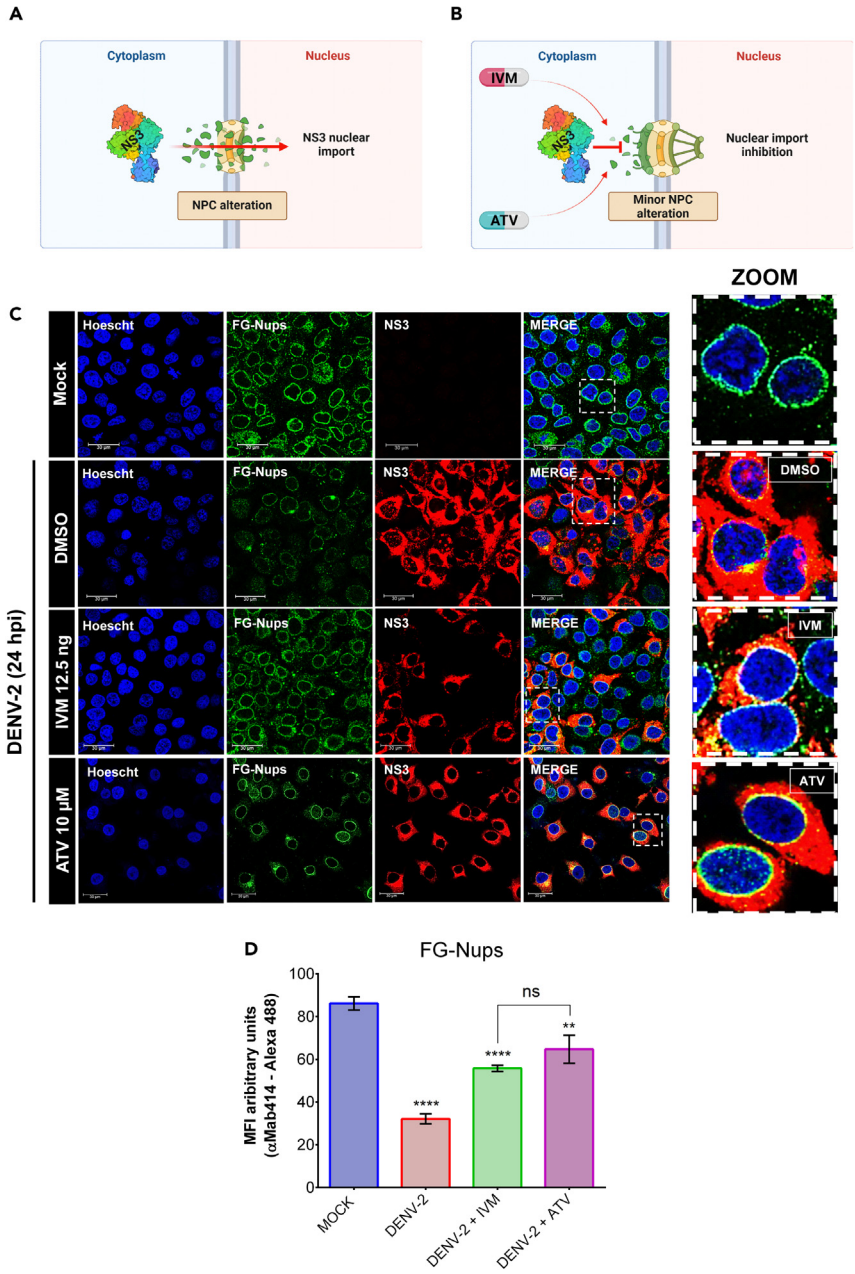

Figure 3. IVM or ATV reduces FG-Nups disruption in Huh7 cells infected with DENV-2

(A and B) Schematic representation of the nuclear pore complex disruption mediated by the presence of NS3 in the nucleus of DENV-2 infected cells.

(C) Confocal microscopy images of cells infected or uninfected with DENV-2 at MOI of 5 and treated with DMSO, 12.5 ng IVM, or 10 μM ATV for 24 h. FG-Nups were labeled with Mab414 antibody, and NS3 protein was labeled as infection control. Scale bar, 30 μm.

(D) The Mean Fluorescence Intensity (MFI) was determined for selected regions of interest (ROIs) in the nucleus and cytoplasm, and the fluorescence ratio nucleus/cytoplasm (Fn/C) was determined for these selected ROIs in each confocal microscopy image (FG-Nups-Alexa488) of cells treated or not with IVM or ATV. n = 40 cells for each condition (in three independent experiments). Data were represented as mean ± standard error of the mean (SEM). Statistical comparison was performed by one-way ANOVA with Tukey post-host tests or two-tailed unpaired Student's t-test. **p 0.035, ****p < 0.0001.

viability (Figure S3A). Consequently, the KPNA1 protein and SV40-NLS localization at 24 h post-treatment in an IVM+ATV combination was evaluated by confocal microscopy. The results demonstrated an increase of KPNA1 protein (Figure 4A) and the SV40-NLS GFP signal (Figure S3C) in the cytoplasm during individual IVM and ATV treatments. Interestingly, combining these drugs enhances the cytoplasmic accumulation of KPNA1 in uninfected cells (Figure 4A), resulting in higher cytoplasmic MFI than individual treatments (Figure 4B). These results showed that the IVM+ATV combination has an additive effect in inhibiting karyopherin nuclear import, which affects the transport of

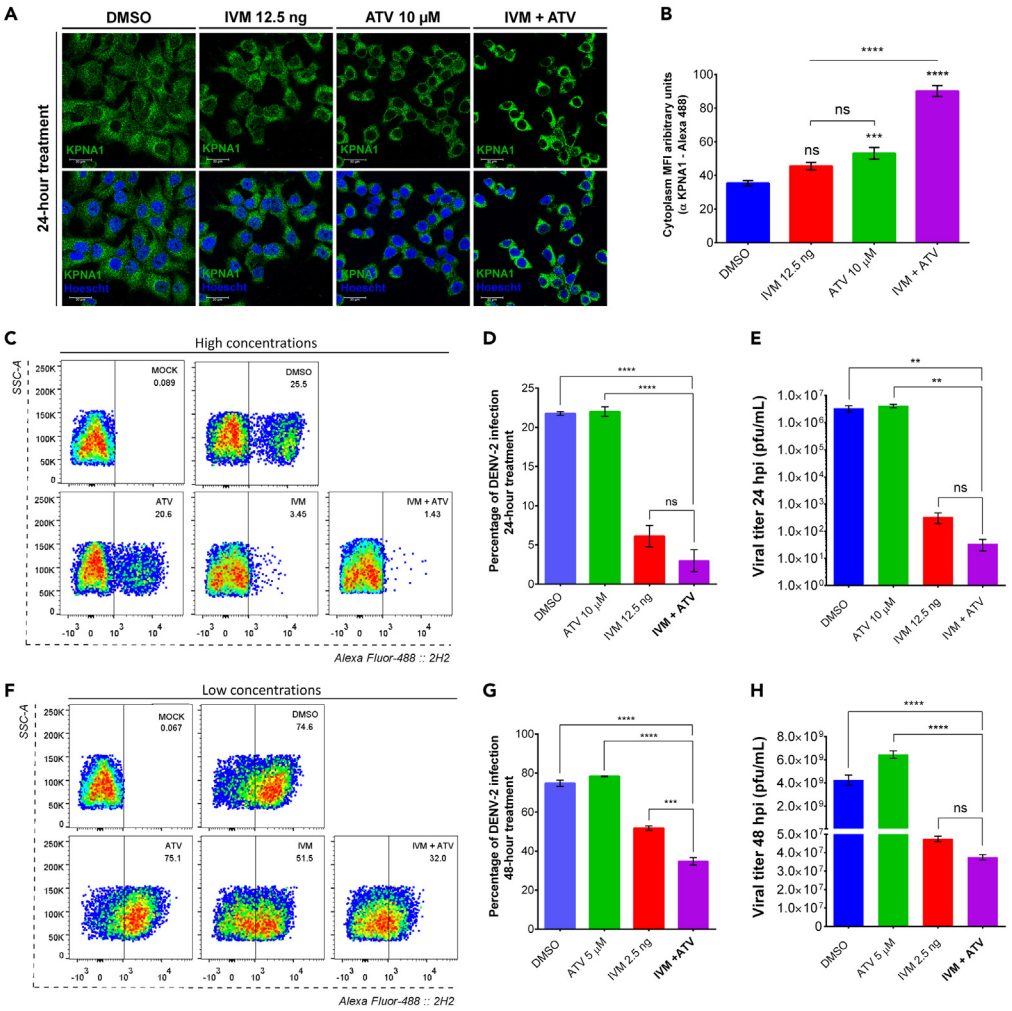

Figure 4. IVM+ATV combination increases KPNA1 protein in the cytoplasm and decreases the percentage of DENV-2 infection

(A) Confocal microscopy images of cells treated with DMSO, 12.5 ng of IVM, 10 μM of ATV, or IVM+ATV combination for 24 h. KPNA1 was labeled to determine the effect of treatment on the nuclear import of cellular proteins. Please see also Figure S3C.

(B) The Mean Fluorescence Intensity (MFI) was determined for selected regions of interest (ROIs) in the cytoplasm. n = 40 cells for each condition (in three independent experiments). Data were represented as mean ± standard error of the mean (SEM). Statistical comparison was performed by one-way ANOVA with Tukey post-host tests. ***p < 0.001, ****p < 0.0001. Scale bar, 30 μm.

Flow cytometry (C and F), percentage of DENV-2 infection (D and G) and viral titer (E and H) in cells uninfected and DENV2 infected cells treated with DMSO or with high (C, D and E) or low concentrations (F, G and H) of IVM or ATV. Cells were infected at MOI of 0.5 for 24 h, and the percentage of infection was analyzed by flow cytometry from three independent experiments in duplicate. The analyzed population evaluates 10,000 events from the total population's single events (SSC-H vs. SSC-A). The events are represented as SSC-A vs. Alexa Fluor 4882H2. Results were expressed as mean ± standard error of the mean (SEM). Statistical comparison was performed by one-way ANOVA with Tukey post-host tests ***p < 0.001, ****p < 0.0001. Please see also Figures S3D and S3E. The viral titer of supernatants from DENV-2 infected cells was determined by plaque assay from three independent experiments. Data were represented as mean ± standard error of the mean (SEM). Statistical comparison was performed by one-way ANOVA with Tukey post-host tests. **p < 0.01, ****p < 0.0001.

importin-dependent proteins (Figure S3C). Based on the inhibitory effect on importin-dependent transport and the anti-DENV effect previously reported for IVM and ATV in monotherapy treatments,[7,39] we decided to evaluate the anti-DENV effect of the IVM+ATV combination. However, viability assays of combined treatments showed that 12.5 ng IVM and 10 μM ATV concentrations were toxic after 24 h (Figure S3B). Therefore, we tested different combination treatment schemes: high concentrations for 24 h (12.5 ng IVM +10 μM ATV) and low concentrations for 48 h (2.5 ng IVM +5 μM ATV).

Flow cytometry assays determined that high concentrations during 24 h significantly reduced the percentage of DENV-2 infection compared to individual IVM or ATV treatments (Figures 4C and 4D). However, these combined concentrations were highly toxic in treatments longer than 24 h but not individually, even at 48 h. (Figure S3D). Therefore, we tested whether the additive antiviral effect of the IVM+ATV combination is maintained at low concentrations at times longer than 24 h.

Interestingly, a significant decrease in the percentage of DENV-2 in infected-cells treated with IVM+ATV at low concentrations at 48 h (Figures 4F and 4G) compared with the treatment with IVM or ATV alone (Figure S3E). Furthermore, we also observed a significant reduction in viral yield at 24 h and 48 h in high and low doses treatment; nevertheless, there was no significant difference between the IVM-treated and combination-treated cells (Figures 4E and 4H). Finally, low concentrations did not significantly reduce the nuclear localization of NS3 or KPNA1 at 12 h of treatment (Figures S3F and S3G). In this regard, our results suggest that the IVM+ATV combination has a significant anti-DENV activity than IVM or ATV alone treatments, even when the cells were treated with low concentrations of these drugs.

Combined ivermectin + atorvastatin treatment has a protective effect in Dengue virus-2-infected AG129 mice

Finally, to confirm the antiviral effect of the combination of IVM+ATV, the AG129 mice knockout for the interferon (IFN) pathway (IFNα/β/γ R−/−) was used. The mice were inoculated intraperitoneally with $4x10^6$ PFU/mL of DENV-2 and treated orally with 4 mg/kg/day of IVM and 20 mg/kg/day of ATV for seven days, both in monotherapy and in combination therapy (Figure S4A) as previously reported.[40–42]

First, to measure the clinical score of each group, we used as reference Table S3 of clinical signs described previously by Farfan & collaborators.[9] No changes were observed in the mean clinical score of the ATV and IVM-treated group compared to the untreated group (Figure S4C). Although ATV monotherapy treatment increased the mean survival time from 18.0 (±1.500) to 20.0 (±1.500) days for untreated and treated mice, respectively, the difference was not significant (Figure S4A). On the other hand, the concentrations used for IVM alone and in the IVM+ATV combination were very toxic for infected mice, with a significant decrease in the percentage survival (Log rank test *p = 0.0177) with a mean survival time of 13 (±1.500) and 17 (±1.225) days, respectively (Figure S4A). These results indicated that 4 mg/kg/day of IVM was highly toxic in monotherapy or combination.

Therefore, lower concentrations of IVM were tested to prevent its toxicity. AG129 mice received one dose of 0.3 mg/kg or 0.6 mg/kg of IVM every other day for ten days (Figure S4D). In addition, the DENV-2 inoculum was increased ($4x10^7$ PFU/mL) to accelerate the symptoms of dengue disease. The results showed that both concentrations increased the mean survival time (Figure S4D) and the percent of survival (Figure S4E) compared to the vehicle-treated group; however, this increase was not statistically significant. Since the treatments delayed the onset of clinical signs, with a greater effect at the 0.6 mg/kg concentration (Figure S4F), this concentration was selected for the combined treatments with 20 mg/kg of ATV.

Female or male mice, uninfected or four days post-infection inoculated with $4x10^7$ PFU/mL of DENV-2, were treated in the following conditions: Vehicle (water), 0.6 mg IVM, 20 mg ATV or the combination of IVM+ATV, for ten days. Mice received five doses of IVM, one every other day, or/and ten doses of ATV, one per day, in single or combined treatments (Figure 5A). Uninfected treated mice were used as the control group (blue) (Figure 5B). We observed that the administration of the drugs did not cause any signs of disease in the uninfected female or male mice (Figures 5B and 5C), so they were classified as "1" according to the table of clinical signs (Table S2).

Clinical signs of DENV-2 infection began 6 days post-infection (dpi) in female mice and 7 dpi in male mice and appeared 2 days later in ATV-treated male mice (day nine post-infection) and three days later in ATV-treated female mice (day nine post-infection) (Figures 5B and 5C). Subsequently, severe signs ("5" according to the table of clinical signs) of disease occurred at 14 dpi in vehicle-treated mice and ATV-treated female mice. In contrast, ATV treatment in male mice delayed severe signs until 18 dpi (Figure 5C).

Notably, IVM and IVM+ATV combination treatments delayed the onset of disease signs by 12 days in male mice and 10 - 9 days in female mice, respectively (Figures 5B and 5C). Interestingly, combined IVM+ATV treatment reduced the onset of severe disease signs up to 22 dpi in male mice, 2 days later than IVM treatment (Figure 5C). However, in female mice, IVM treatment delayed the onset of severe signs by 3 days compared to the group treated with the IVM+ATV combination (from day 20 post-infection to day 23 post-infection) (Figure 5B). These data suggest that treatment with the IVM+ATV combination reduces the onset of severe signs of DENV-2 disease in male AG129 mice but not in female AG129 mice, most likely because single treatment with ATV therapy failed in female mice.

We also evaluated the survival percentage and body weight decline during IVM+ATV treatments. Kaplan-Meier survival curves showed a significant increase in the percentage of survival rate in both genders treated with IVM and IVM+ATV but not in females treated with ATV (Figures 5D and 5E, Table 1). In the total population, the median survival significantly increased from 14 days in untreated mice to 18 and 16 days in mice treated with IVM and IVM+ATV combination, respectively (Table S1). However, the ATV treatment did not increase median survival and, on the contrary, reduced survival in ATV-treated infected females compared to untreated females (Table 1), according to the observed results of the clinical signs. These results suggest that the combined therapy of IVM+ATV has a protective effect, mainly in male mice.

In addition, IVM monotherapy significantly increased the mean survival rate of the total population, including females and males, compared to untreated mice (Figure 6A, Tables 1 and S1). On the other hand, ATV treatment promoted increased mean survival time in male mice but not in females (Figure 6B, Table 1). Moreover, we observed that combined IVM+ATV treatment increased the mean survival time of the total population and treated males compared to untreated mice. However, this increase was not significant in IVM+ATV-treated females (Figure 6C, Table 1). Finally, we observed a lower weight loss in both genders in the groups treated with IVM and IVM+ATV compared to the Vehicle-treated group; nevertheless, we did not detect a significant difference between the treated and untreated groups (Figures S4G and S4H).

Since the combined IVM+ATV treatment had a better effect on male AG129 mice, we measured the viral load in different organs of treated and untreated mice and the nuclear localization of NS3 in tissue sections. Two or three mice per group were infected and treated as described above. Viral load was measured in the livers and brains of mice infected for 8 days at mid-treatment (with three IVM and five ATV doses) (Figure 5A). Interestingly, no viral RNA was found in the livers of the mice. Quantitative real-time PCR (RT-qPCR) data showed significantly lower

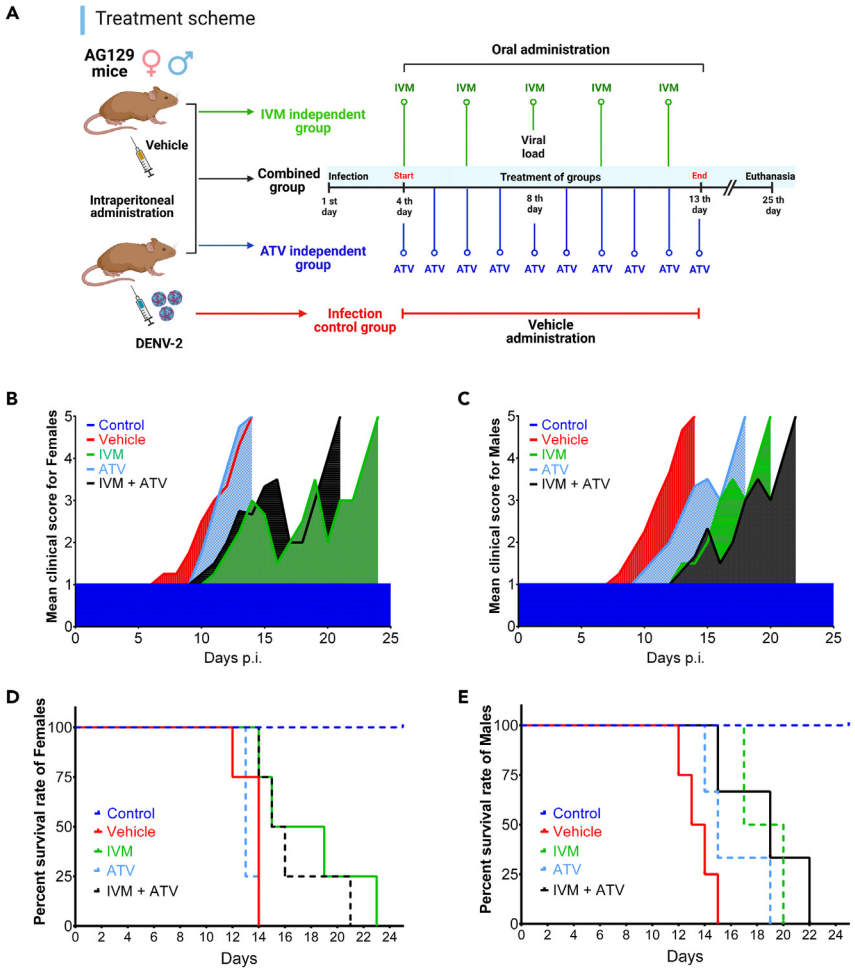

Figure 5. *In vivo* efficacy of IVM+ATV treatment in DENV-2-infected AG129 mice

(A) Workflow for evaluating the effect of combined IVM+ATV treatment in the AG129 mouse model infected with DENV-2. The graphical was elaborated using BioRender.com. Mean clinical scores of AG129 (B) female and (C) male mice infected with DENV-2 treated with Vehicle, IVM, ATV, and IVM+ATV. The morbidity scale is shown in Table S2. Kaplan-Meier survival curves represent the percentage survival of (D) female and (E) male AG129 mice treated with Vehicle, IVM, ATV, and IVM+ATV. The continuous line highlights the treatment that most increased the survival rate compared to the Vehicle. Statistical comparison was performed by Gehan-Breslow Wilcoxon and Log rank (Mantel-Cox) test. p-values are shown in Tables 1 and S1.

viral copies in the brains of AG129 mice treated with the IVM+ATV combination (mean $2.83x10^4$ copies) compared to the other groups (mean Vehicle = $7.5x10^5$ copies, IVM = $4.86x10^5$ copies, and ATV = $3.62x10^5$ copies) (Figure 6D).

Additionally, frozen mouse brain slices were obtained for observation by immunofluorescence. Confocal microscopy images showed infected cells with NS3 protein staining in the cytoplasm and nucleus (Figure 6E), according to our previous *in vitro* results. Interestingly, in the brain tissue of AG129 mice treated with IVM, ATV, and the combination IVM+ATV, we observed a significant reduction of NS3 MFI in the nucleus of infected cells (Figure 6F). Furthermore, during treatment with the IVM+ATV combination, a substantial reduction in NS3 MFI in the cytoplasm was also observed, consistent with the decreased viral load shown above (Figure 6G). These results demonstrate that combined treatment increases survival and reduces DENV-2 viral load in AG129 male mice, suggesting the potential anti-DENV effect of combined IVM+ATV treatment. Besides, we have evidence that IVM and ATV partially impair the nuclear localization of NS3 protein in an *in vivo* model.

DISCUSSION

Finding a treatment or vaccine against dengue disease remains challenging today. Recently, repositioning FDA-approved drugs has proven to help search for new antiviral therapies, interrupting critical cellular processes in the replicative cycle of viruses.[31,43] The advantages of these drugs are that, since they are safe in humans, the development, production, and approval process is avoided; in addition, their therapeutic action and adverse effects are widely known.[44] Recently, the anti-Flavivirus properties of IVM, an anti-parasitic, and ATV, a lipid-lowering drug, have been reported; however, the antiviral mechanisms of both drugs are still under study.[6,39]

Table 1. Combined IVM+ATV treatment on survival of AG129 male and female mice infected with DENV-2

Comparison of treatment groups		# events (n)	Median survival rate (days)	Are the survival rate curves sig different?	Average survival time (days)	Are the average survival times sig different?
Females	Veh **vs.** IVM	Veh = 4 IVM = 4	Veh = 14 IVM = 17	YES Log rank (Mantel-Cox) test ***p = 0.0004 NO Gehan-Breslow Wilcoxon test	Veh = 13.50 IVM = 17.75 ± 1.700	YES ANOVA-LSD *p = 0.0204
	Veh **vs.** ATV	Veh = 4 ATV = 4	Veh = 14 ATV = 13	NO	Veh = 13.50 ATV = 13.25 ± 1.102	NO
	Veh **vs.** IVM + ATV	Veh = 4 IVM+ATV = 4	Veh = 14 IVM+ATV = 15.50	**YES Log rank (Mantel-Cox) test *p= 0.0379 YES Gehan-Breslow Wilcoxon test *p= 0.0398**	Veh = 13.50 IVM+ATV = 16.50 ± 1.742	NO
Males	Veh **vs.** IVM	Veh = 4 IVM = 2	Veh = 13.50 IVM = 18.50	YES Log rank (Mantel-Cox) test *p = 0.0494 NO Gehan-Breslow Wilcoxon test	Veh = 13.50 IVM = 18.50 ± 2.082	YES ANOVA-LSD *p = 0.0252
	Veh **vs.** ATV	Veh = 4 ATV = 3	Veh = 13.50 ATV = 15	NO	Veh = 13.50 ATV = 16 ± 1.191	YES ANOVA-LSD *p = 0.0465
	Veh **vs.** IVM + ATV	Veh = 4 IVM+ATV = 4	Veh = 13.50 IVM+ATV = 19	**YES Log rank (Mantel-Cox) test *p= 0.0409 YES Gehan-Breslow Wilcoxon test *p= 0.0482**	Veh = 13.50 IVM+ATV = 17.50 ± 1.742	YES ANOVA-LSD *p = 0.0300

Summary of statistical data for the *in vivo* assay. Words in bold font are highlighted when both statistical tests *for in vivo* assay studies are statistically significant.

This research proposes the IVM+ATV combination, both FDA-approved drugs, for anti-DENV therapy based on inhibiting nucleus-cytoplasmic transport mechanisms.[37] During the DENV replicative cycle, it has been demonstrated that viral proteins such as C, NS5, and NS3 are transported to the nucleus, which is required for the apoptosis and inhibition of nucleosome formation,[45,46] rewiring host immune response, gene expression,[47,48] nucleoporins degradation and the nuclear pore complex alteration.[38] Due to these findings, studies on using FDA-approved drugs to regulate, inhibit, or understand the dynamics of nuclear localization of DENV proteins have been conducted.[49]

Previous work from our group indicates that DENV-2 and ZIKV NS3 proteins are present in the nucleus and cytoplasm of infected cells at early and late times post-infection.[19,27] In the case of ZIKV NS3, it has been shown to possess an NLS and a NES that favor the nuclear transport of the protein.[27] However, the exact mechanisms for DENV-2 NS3 nucleus-cytoplasm trafficking are unclear. Hence, one of the aims of this study was to determine the pathway used by NS3 to be imported to the nucleus. It has been shown that IVM can inhibit nuclear import by interfering with the Imp αβ1 pathway,[11] a mechanism that prevents the translocation of NS5 RNA-dependent RNA polymerase to the nucleus of flaviviruses.[6,7] On the other hand, for DENV, NS3 has been described to have a putative Imp α/β1-dependent NLS.[19] In this sense, the present study has demonstrated that IVM inhibits the nuclear import of the NS3 protein (Figure 1), suggesting that the Imp α/β1 pathway mediates NS3 transport to the nucleus of infected cells.

ATV, a statin used to treat hypercholesterolemia,[50] also inhibited the nuclear import of NS3 in infected cells (Figure 2E). While Ivermectin inhibits the Imp αβ1 pathway through the dissociation of the Imp α-β1 complex by binding it to the armadillo repeat domain (AMR), affecting its thermal stability,[11] ATV affects the prenylation of GTPases by reducing their membrane localization, involving the organization of the actin cytoskeleton, and affecting intracellular transport.[36] Segatori et al. (2021) reported that importin gene expressions and nuclear accumulation were reduced in uninfected cells treated with IVM and ATV alone or combined.[37] This finding supports our results where KPNA1 is retained in the cytoplasm of ATV-treated Huh7 cells and inhibits nuclear transport of the viral proteins NS3 and NS5 of DENV-2 infected cells (Figure 2). Thus, statins, such as ATV, impair Huh7 cell nuclear transport due to cholesterol depletion by inhibiting the hydroxymethylglutaryl-coenzyme A (HMG-CoA) reductase.[51]

Different studies have shown that the nuclear localization of NS5 prevents interleukin-8 activation and affects cellular mRNA splicing.[52,53] However, not much is known about the role of NS3 in the nucleus. De Jesús-Gonzalez et al. 2020 reported that NS3 of DENV and ZIKV process nucleoporins from NPC.[38,54] During Poliovirus and Rhinovirus infection, nucleoporin degradation has also been associated with viral proteases 2A and 3C,[55,56] suggesting that the nuclear presence of protease 3C is involved in nucleoporins disruption.[57] Therefore, we hypothesized that NS3 can alter the NPC from its nuclear localization (Figure 3A). In this sense, our results indicate that treatment with IVM or ATV reduced the presence of NS3 in the nucleus and the NPC disruption during DENV-2 infection (Figure 3). However, further studies are needed to confirm the importance of the nuclear import of NS3 in NUPs degradation. Thus, our data suggests that inhibiting the nuclear import of viral proteins such as NS3 by IVM and ATV is an attractive target for antiviral design.

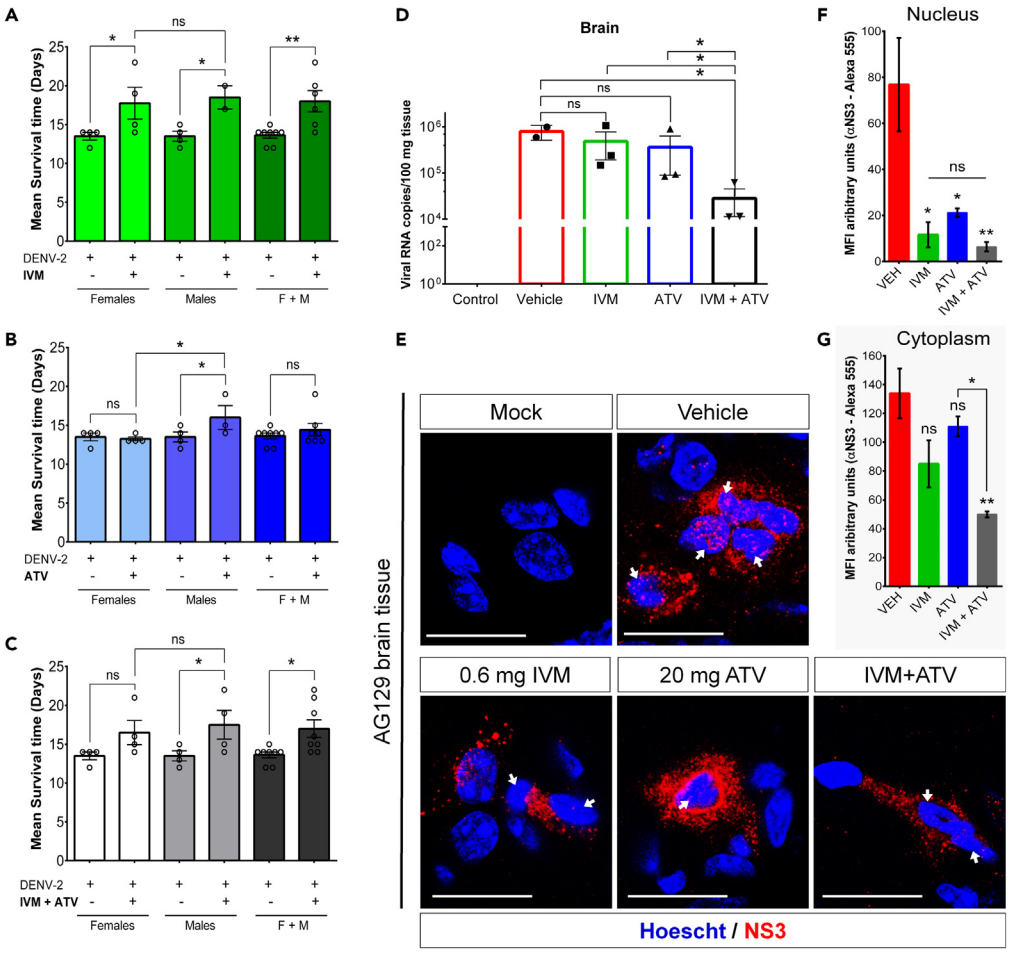

Figure 6. IVM+ATV reduces viral load and nuclear localization of NS3 in the brain of DENV-2-infected AG129 mice

(A–C) Mean survival time of AG129 mice treated with IVM, ATV, and the combination IVM+ATV (n = 6 (2 ♂, 4 ♀), 7 (3 ♂, 4 ♀) and 8 (4 ♂, 4 ♀), respectively). Vehicle-treated mice infected with DENV-2 were used as controls (n = 8 (4 ♂, 4 ♀)). Data were represented as mean ± standard error of the mean (SEM). Statistical comparison was performed by ANOVA-LSD. p-values are shown in Tables 1 and S1.

(D) Effect of IVM, ATV, and IVM+ATV treatments on viral load in brains of DENV-2 infected mice eight days post-infection (n = 3, for each group) compared to vehicle-treated mice (n = 2). Treatment started 4 days post-infection. The independent treated groups received three doses of IVM and five doses of ATV, and the combined group received three doses of IVM+ATV every other day. Data were represented as mean ± standard error of the mean (SEM). Statistical comparison with the vehicle-treated group was performed using the unpaired one-tailed Mann-Whitney test. *p < 0.05.

(E) Brain tissue sections from AG129 male mice. Mice received half of the treatment schedule (five days of treatment). Frozen tissue sections were prepared and labeled with anti-NS3 (viral protein) and Hoescht (nuclei), and the subcellular localization of NS3 was analyzed by confocal microscopy of infected and uninfected mice treated with IVM, ATV, or the combination IVM+ATV. The Mean Fluorescence Intensity (MFI) was determined for selected regions of interest (ROIs) in the (F) nucleus and (G) cytoplasm from mice infected cells of each condition (Vehicle, IVM, ATV or IVM+ATV). Data were represented as mean ± standard error of the mean (SEM). Statistical comparison was performed by one-way ANOVA with Tukey post-host tests. *p 0.05, **p < 0.01.

Previous work demonstrated that IVM pretreatment was sufficient to inhibit NS5 transport, DENV replication, and the helicase activity of the flavivirus NS3 protein.[6,7] Therefore, our results provide additional information about the antiviral effect of IVM: treatments with low concentrations of this drug are not toxic in Huh-7 liver cells (Figure S2B and S2C); this treatment prevents the nuclear import of NS3 (Figure 1), which consequently contributes to reducing the pathogenesis and replication of DENV-2 (Figures 3 and 4). In addition, IVM, in combination with ATV, showed a significant *in vitro* anti-DENV effect compared to monotherapies (Figure 4).

Additionally, our *in vivo* assays performed in immunodeficient AG129 mice, a lethal model for DENV infection,[58] demonstrated that the combined IVM+ATV treatment significantly increased (3 days) the mean survival time in the total population of DENV-2-infected mice (females + males) (Table S1). Furthermore, the Kaplan-Meier survival curves showed a significant increase in survival percentage and a median survival of 6 days longer in IVM+ATV-treated male mice compared to untreated mice (Figure 5 and Table 1). Interestingly, IVM-treated females showed a 3-day increase in mean survival curve compared to the vehicle-treated groups, more significant than the combination treatment, which was only 1.5 days (Table 1). A possible explanation for this is that ATV in the combined treatment affects the survival time of

female mice, as we observed in the ATV-treated female mice group, where there was no difference compared to the mean vehicle survival. (Figure 6).

Previous studies have reported that statins are protective in AG129 mice infected with DENV.[4] However, in this work, ATV treatment only increased the mean survival time in male mice (Figure 6). These effects could be related to the adverse effects of statins in the ovary and uterus[59] and serum androgen depletion.[60] This appears to be an effect of treatments with cholesterol-lowering drugs such as metformin, described by Farfan-Morales et al. (2021).[9] As far as we know, only two clinical trials have studied the role of statins as an antiviral agent for DENV infections, and no evidence of a beneficial effect on clinical manifestations of DENV or viremia in adult patients treated with statins has been found.[61,62] However, no previously mentioned studies have described a differential effect of statins on DENV-infected males and females. Therefore, preclinical and clinical studies should consider the evaluation of statins and any other drugs in gender-divided groups. Finally, we observed that male mice treated with the IVM+ATV combination showed lower viral copy numbers than the other groups (Figure 6) and a delay in the onset of clinical signs of dengue disease (Figure 5). In contrast, clinical trials with IVM in monotherapy showed no clinical efficacy compared to the untreated group but a significant anti-DENV effect.[63]

In this regard, these data might suggest that combination therapy of IVM+ATV could reduce the onset of dengue disease symptoms and viral load, having a substantially better clinical efficacy than monotherapies in patients infected with DENV. However, further studies on cholesterol-lowering drugs in females are needed to demonstrate the effectiveness of combined IVM+ATV therapy. In addition, IVM and ATV have been shown to have immunomodulatory effects.[64,65] Despite this, we emphasize that the anti-DENV effects of the IVM+ATV combination demonstrated in the present *in vivo* study are independent of the IFN-dependent immune response. Hence, with this data, we propose the combination IVM+ATV as a possible antiviral therapy for patients infected with DENV.

Finally, by analysis of histological sections, we found NS3 staining in brain tissue nuclei of male AG129 mice; importantly, we observed a reduction of NS3 MFI in mice treated with IVM, ATV, or the combination IVM+ATV. These data demonstrate the nuclear localization of NS3 in an *in vivo* model and that FDA-approved drugs that can impair nuclear transport reduce the presence of NS3 in the nucleus of tissues from infected AG129 mice. However, further studies are needed to elucidate the role of NS3 in the nucleus in both *in vitro* and *in vivo* models. In summary, inhibiting nuclear transport impairs the nuclear import of DENV proteins and may be a promising target for treating emerging and re-emerging viral diseases.

Limitations of the study

One of the limitations of the study was to evaluate the nuclear transport of NS3 protein in the *in vivo* model, due to the difficulty of controlling the time of infection and the number of infected cells. In addition, there are few methodologies to evaluate nuclear transport in an *in vivo* model. Therefore, further studies are needed to elucidate the transport of viral proteins *in vivo* or in samples from infected patients as well as its role in viral pathogenesis.

STAR★METHODS

Detailed methods are provided in the online version of this paper and include the following:

- KEY RESOURCES TABLE
- RESOURCE AVAILABILITY
  - Lead contact
  - Materials availability
  - Data and code availability
- EXPERIMENTAL MODEL AND STUDY PARTICIPANT DETAILS
  - Cell lines
  - Mice
- METHOD DETAILS
  - Viral infection
  - Transmission immunoelectron microscopy (TIM)
  - Drugs and reagents
  - Cell viability assay
  - Subcellular fractionation and Western blot analysis
  - Transfections experiments
  - Confocal microscopy
  - Flow cytometry assay
  - Viral yield
  - AG129 mouse survival assays
  - Quantification of DENV RNA using RT–qPCR
- QUANTIFICATION AND STATISTICAL ANALYSIS

SUPPLEMENTAL INFORMATION

Supplemental information can be found online at https://doi.org/10.1016/j.isci.2023.108294.

ACKNOWLEDGMENTS

The authors thank Dr. Bulmaro Cisneros from the Department of Genetic and Molecular Biology for donating the plasmid containing NLS-SV40, Dr. Marco Antonio Meraz Ríos and Pilar Figueroa Corona from the Department of Biomedicine for their gentile donation of AG129 mice. Dr. Arely González and Dr. Raymundo Cruz from the Department of Infectomics and Molecular Pathogenesis for obtaining tissue sections, Dr. Bibiana Chávez-Munguía, and Anel E. Lagunes Guillen for their assistance in preparing the electron microscopy image samples. Fernando Medina for their assistance in cell culture, Jaime Zarco and Pablo Gómez from CINVESTAV for technical assistance. This research was supported by CONACYT (Mexico) grants CB-220824 and A1-S-9005 from RMDA and Fundación Miguel Alemán. However, the funders had no role in study design, data collection, analysis, publication decision, or article preparation. In addition, Palacios-Rápalo SN and Cordero-Rivera CD received scholarships from CONACYT.

AUTHOR CONTRIBUTIONS

SP-R and RÁ were responsible for the study design, supervision, and article preparation. CC-R, CF-M, and SP-R were responsible for flow cytometry assays. CF-M and SP-R were responsible for animal experiments. L-DJ and SP-R were responsible for immunofluorescence assays. Finally, RÁ, SP-R, L-DJ, JR-R, CC-R, CF-M, and MM-R were responsible for formal analysis. All authors contributed to the article and approved the submitted version.

DECLARATION OF INTERESTS

The authors declare no competing interests.

INCLUSION AND DIVERSITY

We support inclusive, diverse, and equitable conduct of research.

Received: May 19, 2023
Revised: August 29, 2023
Accepted: October 18, 2023
Published: October 27, 2023

REFERENCES

1. Sanchez, J.D. (2009). OPS/OMS (Pan American Health Organization/World Health Organization).
2. CDC (2019). Dengue Treatment for Healthcare Providers | CDC (Centers for Disease Control and Prevention). https://www.cdc.gov/dengue/healthcare-providers/treatment.html.
3. Pushpakom, S., Iorio, F., Eyers, P.A., Escott, K.J., Hopper, S., Wells, A., Doig, A., Guilliams, T., Latimer, J., McNamee, C., et al. (2019). Drug repurposing: progress, challenges and recommendations. Nat. Rev. Drug Discov. *18*, 41–58. https://doi.org/10.1038/nrd.2018.168.
4. Martinez-Gutierrez, M., Correa-Londoño, L.A., Castellanos, J.E., Gallego-Gómez, J.C., and Osorio, J.E. (2014). Lovastatin delays infection and increases survival rates in AG129 mice infected with dengue virus serotype 2. PLoS One *9*, e87412. https://doi.org/10.1371/journal.pone.0087412.
5. Osuna-Ramos, J.F., Reyes-Ruiz, J.M., Bautista-Carbajal, P., Cervantes-Salazar, M., Farfan-Morales, C.N., De Jesús-González, L.A., Hurtado-Monzón, A.M., and Del Ángel, R.M. (2018). Ezetimibe inhibits dengue virus infection in Huh-7 cells by blocking the cholesterol transporter Niemann-Pick C1-like 1 receptor. Antivir. Res. *160*, 151–164. https://doi.org/10.1016/j.antiviral.2018.10.024.
6. Mastrangelo, E., Pezzullo, M., De Burghgraeve, T., Kaptein, S., Pastorino, B., Dallmeier, K., de Lamballerie, X., Neyts, J., Hanson, A.M., Frick, D.N., et al. (2012). Ivermectin is a potent inhibitor of flavivirus replication specifically targeting NS3 helicase activity: new prospects for an old drug. J. Antimicrob. Chemother. *67*, 1884–1894. https://doi.org/10.1093/jac/dks147.
7. Tay, M.Y.F., Fraser, J.E., Chan, W.K.K., Moreland, N.J., Rathore, A.P., Wang, C., Vasudevan, S.G., and Jans, D.A. (2013). Nuclear localization of dengue virus (DENV) 1–4 non-structural protein 5; protection against all 4 DENV serotypes by the inhibitor Ivermectin. Antivir. Res. *99*, 301–306. https://doi.org/10.1016/j.antiviral.2013.06.002.
8. Wagstaff, K.M., Sivakumaran, H., Heaton, S.M., Harrich, D., and Jans, D.A. (2012). Ivermectin is a specific inhibitor of importin α/β-mediated nuclear import able to inhibit replication of HIV-1 and dengue virus. Biochem. J. *443*, 851–856. https://doi.org/10.1042/BJ20120150.
9. Farfan-Morales, C.N., Cordero-Rivera, C.D., Osuna-Ramos, J.F., Monroy-Muñoz, I.E., De Jesús-González, L.A., Muñoz-Medina, J.E., Hurtado-Monzón, A.M., Reyes-Ruiz, J.M., and Del Ángel, R.M. (2021). The antiviral effect of metformin on zika and dengue virus infection. Sci. Rep. *11*, 8743. https://doi.org/10.1038/s41598-021-87707-9.
10. Johnson-Arbor, K. (2022). Ivermectin: a mini-review. Clin. Toxicol. *60*, 571–575. https://doi.org/10.1080/15563650.2022.2043338.
11. Yang, S.N.Y., Atkinson, S.C., Wang, C., Lee, A., Bogoyevitch, M.A., Borg, N.A., and Jans, D.A. (2020). The broad spectrum antiviral ivermectin targets the host nuclear transport importin α/β1 heterodimer. Antivir. Res. *177*, 104760. https://doi.org/10.1016/j.antiviral.2020.104760.
12. Hiscox, J.A. (2003). The interaction of animal cytoplasmic RNA viruses with the nucleus to facilitate replication. Virus Res. *95*, 13–22. https://doi.org/10.1016/S0168-1702(03)00160-6.
13. Lopez-Denman, A.J., Russo, A., Wagstaff, K.M., White, P.A., Jans, D.A., and Mackenzie, J.M. (2018). Nucleocytoplasmic shuttling of the West Nile virus RNA-dependent RNA polymerase NS5 is critical to infection. Cell Microbiol. *20*, e12848. https://doi.org/10.1111/cmi.12848.
14. Ng, I.H.W., Chan, K.W.-K., Tan, M.J.A., Gwee, C.P., Smith, K.M., Jeffress, S.J., Saw, W.-G., Swarbrick, C.M.D., Watanabe, S., Jans, D.A., et al. (2019). Zika Virus NS5 Forms Supramolecular Nuclear Bodies That Sequester Importin-α and Modulate the Host Immune and Pro-Inflammatory Response in Neuronal Cells. ACS Infect. Dis. *5*, 932–948. https://doi.org/10.1021/acsinfecdis.8b00373.

15. Uchil, P.D., and Satchidanandam, V. (2003). Characterization of RNA synthesis, replication mechanism, and *in vitro* RNA-dependent RNA polymerase activity of japanese encephalitis virus. Virology *307*, 358–371. https://doi.org/10.1016/S0042-6822(02)00130-7.
16. Muramatsu, S., Ishido, S., Fujita, T., Itoh, M., and Hotta, H. (1997). Nuclear localization of the NS3 protein of hepatitis C virus and factors affecting the localization. J. Virol. *71*, 4954–4961.
17. Gagné, B., Tremblay, N., Park, A.Y., Baril, M., and Lamarre, D. (2017). Importin β1 targeting by hepatitis C virus NS3/4A protein restricts IRF3 and NF-κB signaling of IFNB1 antiviral response. Traffic *18*, 362–377. https://doi.org/10.1111/tra.12480.
18. Byk, L.A., and Gamarnik, A.V. (2016). Properties and Functions of the Dengue Virus Capsid Protein. Annu. Rev. Virol. *3*, 263–281. https://doi.org/10.1146/annurev-virology-110615-042334.
19. Palacios-Rápalo, S.N., De Jesús-González, L.A., Reyes-Ruiz, J.M., Osuna-Ramos, J.F., Farfan-Morales, C.N., Gutiérrez-Escolano, A.L., and Del Ángel, R.M. (2021). Nuclear localization of non-structural protein 3 (NS3) during dengue virus infection. Arch. Virol. *166*, 1439–1446. https://doi.org/10.1007/s00705-021-05026-w.
20. Fontoura, B.M., Faria, P.A., and Nussenzveig, D.R. (2005). Viral interactions with the nuclear transport machinery: discovering and disrupting pathways. IUBMB Life *57*, 65–72. https://doi.org/10.1080/15216540500078608.
21. Yarbrough, M.L., Mata, M.A., Sakthivel, R., and Fontoura, B.M.A. (2014). Viral Subversion of Nucleocytoplasmic Trafficking. Traffic *15*, 127–140. https://doi.org/10.1111/tra.12137.
22. Caly, L., Druce, J.D., Catton, M.G., Jans, D.A., and Wagstaff, K.M. (2020). The FDA-approved drug ivermectin inhibits the replication of SARS-CoV-2 *in vitro*. Antivir. Res. *178*, 104787. https://doi.org/10.1016/j.antiviral.2020.104787.
23. Cautain, B., Hill, R., de Pedro, N., and Link, W. (2015). Components and regulation of nuclear transport processes. FEBS J. *282*, 445–462. https://doi.org/10.1111/febs.13163.
24. Chumakov, S.P., and Prassolov, V.S. (2010). Organization and regulation of nucleocytoplasmic transport. Mol. Biol. *44*, 186–201. https://doi.org/10.1134/S0026893310020020.
25. Prikhod'ko, G.G., Prikhod'ko, E.A., Pletnev, A.G., and Cohen, J.I. (2002). Langat Flavivirus Protease NS3 Binds Caspase-8 and Induces Apoptosis. J. Virol. *76*, 5701–5710. https://doi.org/10.1128/JVI.76.11.5701-5710.2002.
26. Reyes-Ruiz, J.M., Osuna-Ramos, J.F., Cervantes-Salazar, M., Lagunes Guillen, A.E., Chávez-Munguía, B., Salas-Benito, J.S., and Del Ángel, R.M. (2018). Strand-like structures and the nonstructural proteins 5, 3 and 1 are present in the nucleus of mosquito cells infected with dengue virus. Virology *515*, 74–80. https://doi.org/10.1016/j.virol.2017.12.014.
27. De Jesús-González, L.A., Palacios-Rápalo, S.N., Reyes-Ruiz, J.M., Osuna-Ramos, J.F., Farfán-Morales, C.N., Cordero-Rivera, C.D., Cisneros, B., Gutiérrez-Escolano, A.L., and del Ángel, R.M. (2022). Nucleo-Cytoplasmic Transport of ZIKV Non-Structural 3 Protein Is Mediated by Importin-α/β and Exportin CRM-1. J. Virol. *97*, e0177322. https://doi.org/10.1128/jvi.01773-22.
28. Soto-Acosta, R., Mosso, C., Cervantes-Salazar, M., Puerta-Guardo, H., Medina, F., Favari, L., Ludert, J.E., and del Angel, R.M. (2013). The increase in cholesterol levels at early stages after dengue virus infection correlates with an augment in LDL particle uptake and HMG-CoA reductase activity. Virology *442*, 132–147. https://doi.org/10.1016/j.virol.2013.04.003.
29. Rothwell, C., Lebreton, A., Young Ng, C., Lim, J.Y.H., Liu, W., Vasudevan, S., Labow, M., Gu, F., and Gaither, L.A. (2009). Cholesterol biosynthesis modulation regulates dengue viral replication. Virology *389*, 8–19. https://doi.org/10.1016/j.virol.2009.03.025.
30. Carro, A.C., and Damonte, E.B. (2013). Requirement of cholesterol in the viral envelope for dengue virus infection. Virus Res. *174*, 78–87. https://doi.org/10.1016/j.virusres.2013.03.005.
31. Farfan-Morales, C.N., Cordero-Rivera, C.D., Reyes-Ruiz, J.M., Hurtado-Monzón, A.M., Osuna-Ramos, J.F., González-González, A.M., De Jesús-González, L.A., Palacios-Rápalo, S.N., and Del Ángel, R.M. (2021). Anti-flavivirus Properties of Lipid-Lowering Drugs. Front. Physiol. *12*, 749770. https://doi.org/10.3389/fphys.2021.749770.
32. Martínez-Gutierrez, M., Castellanos, J.E., and Gallego-Gómez, J.C. (2011). Statins reduce dengue virus production via decreased virion assembly. Intervirology *54*, 202–216. https://doi.org/10.1159/000321892.
33. Krukemyer, J.J., and Talbert, R.L. (1987). Lovastatin: a new cholesterol-lowering agent. Pharmacotherapy *7*, 198–210. https://doi.org/10.1002/j.1875-9114.1987.tb03524.x.
34. Vaziri, N.D., and Liang, K. (2004). Effects of HMG-CoA reductase inhibition on hepatic expression of key cholesterol-regulatory enzymes and receptors in nephrotic syndrome. Am. J. Nephrol. *24*, 606–613. https://doi.org/10.1159/000082510.
35. Farina, H.G., Bublik, D.R., Alonso, D.F., and Gomez, D.E. (2002). Lovastatin alters cytoskeleton organization and inhibits experimental metastasis of mammary carcinoma cells. Clin. Exp. Metastasis *19*, 551–559. https://doi.org/10.1023/a:1020355621043.
36. Chi, X., Wang, S., Huang, Y., Stamnes, M., and Chen, J.-L. (2013). Roles of rho GTPases in intracellular transport and cellular transformation. Int. J. Mol. Sci. *14*, 7089–7108. https://doi.org/10.3390/ijms14047089.
37. Segatori, V.I., Garona, J., Caligiuri, L.G., Bizzotto, J., Lavignolle, R., Toro, A., Sanchis, P., Spitzer, E., Krolewiecki, A., Gueron, G., and Alonso, D.F. (2021). Effect of Ivermectin and Atorvastatin on Nuclear Localization of Importin Alpha and Drug Target Expression Profiling in Host Cells from Nasopharyngeal Swabs of SARS-CoV-2- Positive Patients. Viruses *13*, 2084. https://doi.org/10.3390/v13102084.
38. De Jesús-González, L.A., Cervantes-Salazar, M., Reyes-Ruiz, J.M., Osuna-Ramos, J.F., Farfán-Morales, C.N., Palacios-Rápalo, S.N., Pérez-Olais, J.H., Cordero-Rivera, C.D., Hurtado-Monzón, A.M., Ruíz-Jiménez, F., et al. (2020). The Nuclear Pore Complex: A Target for NS3 Protease of Dengue and Zika Viruses. Viruses *12*, 583. https://doi.org/10.3390/v12060583.
39. Bryan-Marrugo, O.L., Arellanos-Soto, D., Rojas-Martinez, A., Barrera-Saldaña, H., Ramos-Jimenez, J., Vidaltamayo, R., and Rivas-Estilla, A.M. (2016). The anti-dengue virus properties of statins may be associated with alterations in the cellular antiviral profile expression. Mol. Med. Rep. *14*, 2155–2163. https://doi.org/10.3892/mmr.2016.5519.
40. Ketkar, H., Yang, L., Wormser, G.P., and Wang, P. (2019). Lack of efficacy of ivermectin for prevention of a lethal Zika virus infection in a murine system. Diagn. Microbiol. Infect. Dis. *95*, 38–40. https://doi.org/10.1016/j.diagmicrobio.2019.03.012.
41. Hussein, H.M., Al-Khoury, D.K., Abdelnoor, A.M., and Rahal, E.A. (2019). Atorvastatin increases the production of proinflammatory cytokines and decreases the survival of Escherichia coli-infected mice. Sci. Rep. *9*, 11717. https://doi.org/10.1038/s41598-019-48282-2.
42. Mancini, G., Martins, W.C., de Oliveira, J., de Bem, A.F., and Tasca, C.I. (2020). Atorvastatin Improves Mitochondrial Function and Prevents Oxidative Stress in Hippocampus Following Amyloid-β1-40 Intracerebroventricular Administration in Mice. Mol. Neurobiol. *57*, 4187–4201. https://doi.org/10.1007/s12035-020-02026-w.
43. Punekar, M., Kasabe, B., Patil, P., Kakade, M.B., Parashar, D., Alagarasu, K., and Cherian, S. (2022). A Transcriptomics-Based Bioinformatics Approach for Identification and In Vitro Screening of FDA-Approved Drugs for Repurposing against Dengue Virus-2. Viruses *14*, 2150. https://doi.org/10.3390/v14102150.
44. Ashburn, T.T., and Thor, K.B. (2004). Drug repositioning: identifying and developing new uses for existing drugs. Nat. Rev. Drug Discov. *3*, 673–683. https://doi.org/10.1038/nrd1468.
45. Netsawang, J., Noisakran, S., Puttikhunt, C., Kasinrerk, W., Wongwiwat, W., Malasit, P., Yenchitsomanus, P.t., and Limjindaporn, T. (2010). Nuclear localization of dengue virus capsid protein is required for DAXX interaction and apoptosis. Virus Res. *147*, 275–283. https://doi.org/10.1016/j.virusres.2009.11.012.
46. Colpitts, T.M., Barthel, S., Wang, P., and Fikrig, E. (2011). Dengue Virus Capsid Protein Binds Core Histones and Inhibits Nucleosome Formation in Human Liver Cells. PLoS One *6*, e24365. https://doi.org/10.1371/journal.pone.0024365.
47. Petit, M.J., Kenaston, M.W., Pham, O.H., Nagainis, A.A., Fishburn, A.T., and Shah, P.S. (2021). Nuclear dengue virus NS5 antagonizes expression of PAF1-dependent immune response genes. PLoS Pathog. *17*, e1010100. https://doi.org/10.1371/journal.ppat.1010100.
48. Giovannoni, F., Ladelfa, M.F., Monte, M., Jans, D.A., Hemmerich, P., and García, C. (2019). Dengue Non-structural Protein 5 Polymerase Complexes With Promyelocytic Leukemia Protein (PML) Isoforms III and IV to Disrupt PML-Nuclear Bodies in Infected Cells. Front. Cell. Infect. Microbiol. *9*, 284.
49. Yang, S.N.Y., Maher, B., Wang, C., Wagstaff, K.M., Fraser, J.E., and Jans, D.A. (2022). High Throughput Screening Targeting the Dengue NS3-NS5 Interface Identifies Antivirals against Dengue, Zika and West Nile Viruses. Cells *11*, 730. https://doi.org/10.3390/cells11040730.
50. Gentile, S., Turco, S., Guarino, G., Sasso, C.F., Amodio, M., Magliano, P., Salvatore, T., Corigliano, G., Agrusta, M., De Simone, G., et al. (2000). Comparative efficacy study of atorvastatin vs simvastatin, pravastatin, lovastatin and placebo in type 2 diabetic patients with hypercholesterolaemia.

Diabetes Obes. Metab. *2*, 355–362. https://doi.org/10.1046/j.1463-1326.2000.00106.x.

51. Mahmoudi, M., Gorenne, I., Mercer, J., Figg, N., Littlewood, T., and Bennett, M. (2008). Statins Use a Novel Nijmegen Breakage Syndrome-1–Dependent Pathway to Accelerate DNA Repair in Vascular Smooth Muscle Cells. Circ. Res. *103*, 717–725. https://doi.org/10.1161/CIRCRESAHA.108.182899.
52. Rawlinson, S.M., Pryor, M.J., Wright, P.J., and Jans, D.A. (2009). CRM1-mediated nuclear export of dengue virus RNA polymerase NS5 modulates interleukin-8 induction and virus production. J. Biol. Chem. *284*, 15589–15597. https://doi.org/10.1074/jbc.M808271200.
53. De Maio, F.A., Risso, G., Iglesias, N.G., Shah, P., Pozzi, B., Gebhard, L.G., Mammi, P., Mancini, E., Yanovsky, M.J., Andino, R., et al. (2016). The Dengue Virus NS5 Protein Intrudes in the Cellular Spliceosome and Modulates Splicing. PLoS Pathog. *12*, e1005841. https://doi.org/10.1371/journal.ppat.1005841.
54. De Jesús-González, L.A., Palacios-Rápalo, S., Reyes-Ruiz, J.M., Osuna-Ramos, J.F., Cordero-Rivera, C.D., Farfan-Morales, C.N., Gutiérrez-Escolano, A.L., and Del Ángel, R.M. (2021). The Nuclear Pore Complex Is a Key Target of Viral Proteases to Promote Viral Replication. Viruses *13*, 706. https://doi.org/10.3390/v13040706.
55. Sharma, R., Raychaudhuri, S., and Dasgupta, A. (2004). Nuclear entry of poliovirus protease-polymerase precursor 3CD: implications for host cell transcription shut-off. Virology *320*, 195–205. https://doi.org/10.1016/j.virol.2003.10.020.
56. Tian, W., Cui, Z., Zhang, Z., Wei, H., and Zhang, X. (2011). Poliovirus 2Apro induces the nucleic translocation of poliovirus 3CD and 3C′ proteins. Acta Biochim. Biophys. Sin. *43*, 38–44. https://doi.org/10.1093/abbs/gmq112.
57. Walker, E., Jensen, L., Croft, S., Wei, K., Fulcher, A.J., Jans, D.A., and Ghildyal, R. (2016). Rhinovirus 16 2A Protease Affects Nuclear Localization of 3CD during Infection. J. Virol. *90*, 11032–11042. https://doi.org/10.1128/JVI.00974-16.
58. Sarathy, V.V., Milligan, G.N., Bourne, N., and Barrett, A.D.T. (2015). Mouse models of dengue virus infection for vaccine testing. Vaccine *33*, 7051–7060. https://doi.org/10.1016/j.vaccine.2015.09.112.
59. Jiao, X.F., Li, H.L., Jiao, X.Y., Guo, Y.C., Zhang, C., Yang, C.S., Zeng, L.N., Bo, Z.Y., Chen, Z., Song, H.B., and Zhang, L.L. (2020). Ovary and uterus related adverse events associated with statin use: an analysis of the FDA Adverse Event Reporting System. Sci. Rep. *10*, 11955. https://doi.org/10.1038/s41598-020-68906-2.
60. Cassidy-Vu, L., Joe, E., and Kirk, J.K. (2016). Role of Statin Drugs for Polycystic Ovary Syndrome. J. Family Reprod. Health *10*, 165–175.
61. Whitehorn, J., Nguyen, C.V.V., Khanh, L.P., Kien, D.T.H., Quyen, N.T.H., Tran, N.T.T., Hang, N.T., Truong, N.T., Tai, L.T.H., Huong, N.T.C., et al. (2016). Lovastatin for the Treatment of Adult Patients with Dengue: A Randomized, Double-Blind, Placebo-Controlled Trial. Clin. Infect. Dis. *62*, 468–476. https://doi.org/10.1093/cid/civ949.
62. Chia, P.Y., Htun, H.L., Ling, W.P., Leo, Y.S., Yeo, T.W., and Lye, D.C.B. (2018). Hyperlipidemia, statin use and dengue severity. Sci. Rep. *8*, 17147. https://doi.org/10.1038/s41598-018-35334-2.
63. Suputtamongkol, Y., Avirutnan, P., Mairiang, D., Angkasekwinai, N., Niwattayakul, K., Yamasmith, E., Saleh-Arong, F.A.H., Songjaeng, A., Prommool, T., Tangthawornchaikul, N., et al. (2021). Ivermectin Accelerates Circulating Nonstructural Protein 1 (NS1) Clearance in Adult Dengue Patients: A Combined Phase 2/3 Randomized Double-blinded Placebo Controlled Trial. Clin. Infect. Dis. *72*, e586–e593. https://doi.org/10.1093/cid/ciaa1332.
64. Blankier, S., McCrindle, B.W., Ito, S., and Yeung, R.S.M. (2011). The role of atorvastatin in regulating the immune response leading to vascular damage in a model of Kawasaki disease. Clin. Exp. Immunol. *164*, 193–201. https://doi.org/10.1111/j.1365-2249.2011.04331.x.
65. Uematsu, T., Takano, T., Matsui, H., Kobayashi, N., Ōmura, S., and Hanaki, H. (2023). Prophylactic administration of ivermectin attenuates SARS-CoV-2 induced disease in a Syrian Hamster Model. J. Antibiot. *76*, 481–488. https://doi.org/10.1038/s41429-023-00623-0.
66. Prada-Arismendy, J., Rincón, V., and Castellanos, J.E. (2012). Comparative Evaluation of Permissiveness to Dengue Virus Serotype 2 Infection in Primary Rodent Macrophages. J. Trop. Med *2012*, e950303. https://doi.org/10.1155/2012/950303.
67. Hashemi, A., Roohvand, F., Ghahremani, M.H., Aghasadeghi, M.R., Vahabpour, R., Motevau, F., and Memarnejadian, A. (2012). Optimization of transfection methods for Huh-7 and Vero cells: comparative study. Tsitol. Genet. *46*, 19–27.
68. Morens, D.M., Halstead, S.B., Repik, P.M., Putvatana, R., and Raybourne, N. (1985). Simplified plaque reduction neutralization assay for dengue viruses by semimicro methods in BHK-21 cells: comparison of the BHK suspension test with standard plaque reduction neutralization. J. Clin. Microbiol. *22*, 250–254. https://doi.org/10.1128/jcm.22.2.250-254.1985.
69. Orozco, S., Schmid, M.A., Parameswaran, P., Lachica, R., Henn, M.R., Beatty, R., and Harris, E. (2012). Characterization of a model of lethal dengue virus 2 infection in C57BL/6 mice deficient in the alpha/beta interferon receptor. J. Gen. Virol. *93*, 2152–2157. https://doi.org/10.1099/vir.0.045088-0.
70. Angel-Ambrocio, A.H., Soto-Acosta, R., Tammineni, E.R., Carrillo, E.D., Bautista-Carbajal, P., Hernández, A., Sánchez, J.A., and del Angel, R.M. (2015). An embryonic heart cell line is susceptible to dengue virus infection. Virus Res. *198*, 53–58. https://doi.org/10.1016/j.virusres.2015.01.004.

STAR★METHODS

KEY RESOURCES TABLE

REAGENT or RESOURCE	SOURCE	IDENTIFIER
Antibodies		
Mouse anti-KPNA1	Santa Cruz	Cat# sc-517105; RRID: AB_2721174
Mouse anti-KPNA2	Santa Cruz	Cat# sc-136204; RRID: AB_10709746
Mouse anti-GAPDH	Santa Cruz	Cat# sc-47724; RRID: AB_627678
Mouse anti-lamina A/C	Santa Cruz	Cat# sc-376248; RRID: AB_10991536
Mouse anti-calreticulin	Santa Cruz	Cat# sc-6468; RRID: AB_667960
Rabbit anti-NS3	GENETEX	Cat# GTX124252; RRID: AB_11171668
Rabbit anti-NS5	GENETEX	Cat# GTX124253; RRID: AB_11169932
HRP-conjugated goat anti-mouse	Cell Signaling	Cat# 7076S; RRID: AB_331144
HRP-conjugated goat anti-rabbit	Cell Signaling	Cat# 7074S; RRID: AB_2099234
Goat anti-mouse Alexa Fluor 488	Invitrogen	Cat# A21202;RRID: AB_141607
Goat anti-rabbit Alexa Fluor 555	Invitrogen	Cat# A21428; RRID: AB_2535849
Bacterial and virus strains		
DENV-2 New Guinea C Strain	Kindly donated by Instituto de Diagnóstico y Referencia Epidemiológicos Dr. Manuel Martínez Báez (InDRE), Mexico.	N/A
Chemically Competent *E. coli* DH5α	Invitrogen	Cat# 18265-017
Chemicals, peptides, and recombinant proteins		
DMEM	Gibco	Cat# 12491-015
MEM	Gibco	Cat# 41500-015
HANK's balanced salt solution	Gibco	Cat# 24020-117
Ivermectin	Sigma-Aldrich	Cat# I8898-250MG
Veridex (Ivermectin)	Laboratorios Maver de México	N/A
APOTEX (Atorvastatin)	PROTEIN S.A DE C.V. México	N/A
Super Signal West Femto Chemiluminescent Substrate	Thermo Scientific	Cat# 34095
OptiMem	Gibco	Cat# 11058-021
TRIzol reagent	Invitrogen	Cat# 15596026.PPS
DNAse1	BioLabs	Cat# M0303
Critical commercial assays		
3-(4,5- dimethylthiazol-2-yl)-2,5 diphenyltetrazolium bromide (MTT)	Sigma-Aldrich	Cat# M5655-500MG
Cell Fractionation Kit	Abcam	Cat# ab109719
SYBR Green PCR-Master mix	BIO-RAD	Cat# 172-5150
Zippy Plasmid Miniprep kit	ZYMO Research	Cat# D4019
Reverse transcriptase M-MLV	Invitrogen	Cat# 28025-013
Experimental models: Cell lines		
Huh-7	Kindly donated by Dr. Rivas from Universidad Autonoma de Nuevo Leon, Mexico.	N/A
BHK-21	Kindly donated by Instituto de Medicina Tropical "Pedro Kourí", Cuba.	N/A

(*Continued on next page*)

Continued

REAGENT or RESOURCE	SOURCE	IDENTIFIER
Experimental models: Organisms/strains		
CD-1 mice: ICR-CD1, Strain Code: 022.	Charles River Laboratories	N/A
AG129 mice: strain 129/Sv mice doubly deficient in IFN-α/β and -γ receptors	La Jolla Institute for Allergy and Immunology	N/A
Oligonucleotides		
Primer DENV Capsid gene Forward: 5′-CAATATGCTGAAACGCGAGA-3′	Prada-Arismendy et al.[66]	N/A
Primer DENV Capsid gene Reverse: 5′-TGCTGTTGGTGGGATTGTTA-3′	Prada-Arismendy et al.[66]	N/A
Recombinant DNA		
pcDNA_DENV2-NS2B3_V5	Addgene	Cat# 115906
NLS-SV40-4GFP	Kindly donated by Dr. Bulmaro Cisneros from Department of Genetic and Molecular Biology-CINVESTAV	N/A
Software and algorithms		
ImageJ	ImageJ	https://imagej.nih.gov/ij/
Icy image analysis	Chaumont, F. et al.	https://icy.bioimageanalysis.org
GraphPad Prism 6.0	GraphPad Software, San Diego California USA	https://www.graphpad.com
FlowJo v. 10 software	BD Life Sciences	https://www.flowjo.com/solutions/flowjo
Leica Application Suite X Core v3.3.0	Leica	https://www.leica-microsystems.com/products/microscope-software/details/product/leica-las-x-ls/

RESOURCE AVAILABILITY

Lead contact

Further information and requests for resources and reagents should be directed to and will be fulfilled by the lead contact Rosa María Del Ángel (rmangel@cinvestav.mx).

Materials availability

This study did not generate new unique reagents.

Data and code availability

- All original data reported in this paper will be shared by the lead contact upon request.
- This paper does not report original code.
- Any additional information required to reanalyze the data reported in this paper is available from the lead contact upon request.

EXPERIMENTAL MODEL AND STUDY PARTICIPANT DETAILS

Cell lines

The human hepatocellular carcinoma cell line Huh-7 was grown in advance Dulbeccós Modified Eagle Medium (DMEM) (complete medium) supplemented with 2 mM glutamine, 7% fetal bovine serum (FBS), high glucose (4 g/L), Amphotericin B (1000X), penicillin (50 U/mL) and streptomycin (50 μg/mL) at 37°C and a 5% CO_2 humidified atmosphere. Baby hamster kidney-21 (BHK-21) cells were maintained in MEM supplemented with 8% FBS, high glucose (4 g/L), penicillin (50 U/mL) and streptomycin (50 μg/mL) at 37°C and a 5% CO_2 humidified atmosphere.

Mice

The animal experiment followed the Official Mexican Standard Guidelines for Production, Care, and Use of Laboratory Animals (NOM-062-ZOO-1999). The protocol 048-02, was approved by the Animal Care and Use Committee (CICUAL) at CINVESTAV-IPN, Mexico. AG129 mice (strain 129/Sv) (6-8-week-old, female or male) were kindly donated by Dr. Marco Antonio Meraz Ríos (Biomedicine Department, Center for Research and Advanced Studies (CINVESTAV-IPN, Mexico)), which were provided by the La Jolla Institute for Allergy and Immunology.

Neonatal CD1 (ICR-CD1, Strain Code: 022) and AG129 mice were bred and housed at the Laboratory Animal Production and Experimentation Unit (UPEAL-CINVESTAV).

METHOD DETAILS

Viral infection

DENV-2 (New Guinea C strain) was kindly donated by Instituto de Diagnóstico y Referencia Epidemiológicos Dr. Manuel Martínez Báez (InDRE), Mexico. DENV-2 was propagated using CD-1 suckling mice brains (provided by the Laboratory Animal Production and Experimentation Unit (UPEAL). The uninfected CD-1 suckling mice brain extracts were used as control (Mock-infected). Huh-7 cells seeded at 80% of confluence were infected with DENV-2 at a multiplicity of infection of 0.5, 5, and 10 in HANK's balanced salt solution for 2 hours (h) at 37°C. Later, the infection was allowed to proceed for 12 h, 24 h, 36 h, or 48 h.

Transmission immunoelectron microscopy (TIM)

The Huh7 cells grown in p100 dishes were infected with mock or DENV-2 at an MOI of 10. After 12 h or 24 h, the cells were fixed with 4% paraformaldehyde/0.5% glutaraldehyde for 1 h at room temperature (RT), dehydrated with increasing concentrations of ethanol, embedded in the acrylic resin (LR White), and polymerized under UV irradiation at 4°C overnight. Resin-embedded cell sections of 70 nm were mounted on Formvar-covered nickel grids and incubated in PBS with 10% FBS for 1 h to block nonspecific binding and reacted with an anti-NS3 antibody diluted 1:20 in PBS with 5% FBS. The samples were washed three times and incubated with an anti-rabbit IgG secondary antibody conjugated to 20-nm colloidal gold particles (Ted Pella Inc., Redding, CA, USA) at RT for 1 h. Finally, the sections were contrasted with uranyl acetate and lead citrate before being examined under a Jeol JEM-1011 transmission electron microscope (Jeol Ltd., Tokyo, Japan).

Drugs and reagents

IVM (Sigma) and ATV (APOTEX) compounds were first resuspended in dimethyl sulfoxide (DMSO) at concentrations of 2.5 mg/mL and 20 mM/mL, respectively, then aliquoted and stored at -20°C. Final working concentrations were achieved after serial dilutions using DMSO. Control cells were treated with DMSO as a Vehicle. For *in vivo* assay, groups were administered with Veridex (Ivermectin) and APOTEX (Atorvastatin) resuspended in sterile water (Vehicle).

Cell viability assay

The effects of IVM and ATV on Huh7 cell viability were measured using the 3-(4,5- dimethylthiazol-2-yl)-2,5 diphenyltetrazolium bromide (MTT) assay (Sigma-Aldrich). Briefly, cells were plated in 96-well flat bottom plates in complete DMEM and allowed to attach overnight. The Huh7 cells were treated for 24 h, or 48 h with increasing concentrations of IVM (12 μM, 25 μM, 50 μM, 75 μM, or 100 μM) or with increasing concentrations of ATV (5 μM, 10 μM, 15 μM, 20 μM or 50 μM). The IVM+ATV combination assay was performed using high and low concentrations of IVM and ATV that showed a viability percentage above 80% at 24 h or 48 h. After adding 10 μL of MTT reagent to each well, the plates were incubated for 3 h. Formazan crystals were solubilized using DMSO, and each well's absorbance was measured at 562 nm and 630 nm to eliminate the background. The vehicle-treated control cells' optical density was 100% viability.

Subcellular fractionation and Western blot analysis

The Huh7 cells grown in 6-well plates at 80% or 90% were infected with mock or DENV-2 for 24 h. Then, the Huh7 cells were washed 3 times using cold 1X PBS, and the cells were fractionated following the Abcam Cell Fractionation Kit (ab109719) instructions. The cytoplasmic and nuclear fractions were stored at -80°C until use. The extracts from cytoplasmic fractions were quantified using the BCA Protein Assay (Thermo Scientific). SDS-PAGE separated thirty micrograms of protein, transferred to nitrocellulose membranes (Bio-Rad), and blocked with 10% nonfat milk in PBST (1X PBS/0.01% Triton X-100) for 1 h at RT. The immunoblotting was performed with the mouse anti-KPNA1 (1:1000; sc-517105), mouse anti-KPNA2 (1:1000; sc-136204), mouse anti-GAPDH (1:1000; sc-47724), mouse anti-lamina A/C (LMNA 1:1500; sc-376248) as nuclear fraction control or mouse anti-calreticulin (CRT) polyclonal antibody (1:1500; sc-6468) as cytoplasmic fraction control. HRP-conjugated goat anti-mouse or anti-rabbit IgG antibodies (1:5000; Cell Signaling) with 5% nonfat milk in PBST were used as secondary antibodies. The proteins were visualized using the Super Signal West Femto Chemiluminescent Substrate (Thermo Scientific), and the densitometric analysis was performed with the ImageJ software.

Transfections experiments

Plasmid containing the sequence of DENV-2 NS2B3 protein (pcDNA_DENV2-NS2B3_V5) was a gift from Alan Rothman (Addgene plasmid # 115906; http://n2t.net/addgene:115906; RRID: Addgene_115906) and a plasmid containing NLS-SV40 with four green fluorescent protein (GFP) was kindly donated by Dr. Bulmaro Cisneros from Department of Genetic and Molecular Biology, Center for Research and Advanced Studies (CINVESTAV-IPN, Mexico). These plasmids were propagated in competent *E. coli* DH5α (Invitrogen), and the purification was performed using the Zippy Plasmid Miniprep kit (ZYMO Research), following the instructions provided by the manufacturer.

Huh7 cells were transfected with plasmids at a confluence of 70%–80% using electroporation following the Hashemi et al. 2012[67] protocol, with some modifications. Briefly, $1x10^7$ cells were washed with cold 1X PBS and resuspended in 100 μL of OptiMem with 5 μg of DNA. The cells were transferred to a Gene Pulser cuvette with a 4mm electrode gap. The electroporation was performed on a Gene Pulser Xcell (BioRad, Germany), with electric field strength and pulse length of 170 V and 40 ms in exponential decay. Cells were cultured in advanced DMEM with 15% FBS, and transfection was evaluated at 48 h by confocal microscopy.

Confocal microscopy

The Huh7 cells grown at 70-80% of confluence on coverslips placed in 24-well plates were mock-infected or infected with DENV-2 for 12 h or 24 h. In addition, frozen brain tissue sections from AG129 mice treated or untreated were prepared at a thickness of 0.8 μm. The Huh7 infected cells, transfected cells, or tissue sections were washed three times with 1X PBS, fixed with 4% paraformaldehyde (PFA) for 30 min, and permeabilized (0.2% saponin, 1% FBS and 1X PBS) for 30 min. Later, the cells were incubated overnight at 4°C with rabbit polyclonal anti-NS3 antibody (1:200; GENETEX: GTX 124252), rabbit anti-NS5 (1:200; GENETEX: GTX124253), mouse anti prM/E (2H2) or mouse anti-KPNA1 (1:100; sc-517105). As secondary antibodies, goat anti-mouse Alexa Fluor 488 and goat anti-rabbit Alexa Fluor 555 (Life Technologies) were used, and the nuclei were counterstained with Hoechst (Santa Cruz). The slides were observed on a Leica TCS SP8 Confocal Microscope (Leica Microsystems), and the images were analyzed with the Leica Application Suite X Core Offline v3.3.0 software.

Flow cytometry assay

The infected untreated and treated cells were analyzed by flow cytometry to determine the percentage of infected cells. The antibody 2H2 was used to determine the percentage of infected cells by flow cytometry. A goat anti-mouse Alexa Fluor 488 was used as a secondary antibody (Life Technologies). The Flow cytometry assay was performed in a BD LSR Fortessa, and the data were analyzed using the FlowJo v. 10 software. Three independent experiments in duplicate were performed to determine the percentage of infected cells.

Viral yield

Supernatants from the DENV-2 infected untreated and treated cells were used to determine the viral yield using plaque-forming units (PFU) modified assay of Morens et al.[68] Three independent experiments in duplicate were performed for each assay.

AG129 mouse survival assays

The AG129 mice were infected with $4x10^6$ or $4x10^7$ PFU/mL of DENV-2 per mouse. The virus was inoculated intraperitoneally in 100 μL of injectable water. According to the literature, the IVM-treated group received 4 mg, 0.6 mg, or 0.3 mg/kg/day of the drug, and the ATV-treated group received 20 mg/kg/day using an oral tube. The treatments started from day four post-infection for seven or ten days. The mice's weight and the clinical signs of the disease were monitored daily until the day of euthanasia. The signs of the disease are based on a clinical score reported by Orozco et al.[69] to monitor the average morbidity of DENV-infected mice on a scale of 1 to 5, where "1" represents healthy and "5" moribund mice (Table S3). Two independent essays of 2 or 4 mice each were performed. Mice that died from causes other than infection were excluded. The survival results, the clinical score, and the mouse weight were plotted and analyzed using Graph Pad Prism software version 6.0.

Quantification of DENV RNA using RT–qPCR

Brains from male AG129 mice uninfected or infected with DENV-2 and treated with Vehicle, IVM, ATV, or IVM+ATV were used to measure viral load. Briefly, total RNA was extracted 100 mg of the brain from 2 or 3 mice per condition (each mouse was considered one experimental unit.) using TRIzol reagent (Invitrogen Cat. 15596026.PPS) following the manufacturer's specifications. Next, samples were treated with DNAse 1 (BioLabs Cat. M0303) following the manufacturer's instructions. Next, 1 μg total RNA was reverse transcribed to cDNA using Reverse transcriptase M-MLV (Invitrogen). Finally, from 200 ng of cDNA, quantitative polymerase chain reaction (qPCR) was performed to quantify DENV-2 viral RNA copies from mouse brains, using the following primers: Fw: 5′-CAATATGCTGAAACGCGAGA-3′, Rv: 5′-TGCTGTTGGTGGGATTGTTA-3′).[66]

For each PCR reaction, 5 μl of SYBR Green PCR-Master mix (iTaq™ Universal SYBR Green One-Step Kit, BIO-RAD Cat. 172-5150), 0.5 μl of each primer 10 μM, and 2 μl of cDNA diluted in RNase-free water were added. Thermal cycling conditions were as follows: Initial step at 50°C for 2 min, then 95°C for 1 min, followed by 40 cycles of 95°C for 10 sec and 60°C for 30 sec, using the Eco Illumina System equipment. In parallel, we performed a standard curve (10^8, 10^7, 10^6, 10^5, 10^4, 10^3, 10^2) from a plasmid possessing a 151 bp insert of the DENV-2 genome (NCBI ID: NC_001474.2) corresponding to the C protein region,[70] which was amplified with the same primers mentioned above. The threshold was adjusted with a mock-infected mouse sample and the non-templated control. The results were analyzed with EcoStudy software version 5.04890. Data were expressed as viral copies in 100 mg of tissue.

QUANTIFICATION AND STATISTICAL ANALYSIS

Images obtained by confocal microscopy were analyzed using the Icy image analysis software. Three different images for each condition were imported, and the mean fluorescence intensity (MFI) for pixel values was obtained for every selected region of interest (ROI) to quantify the

nuclear fluorescence (Fn) concerning the cytoplasm fluorescence (Fc). The Fn/C ratio was determined according to Fn/Fc = (Fn-Fb)/Fc-Fb), where Fb was the black-ground fluorescence.[13] MFI arbitrary units of Fn/C were expressed as the mean, and the standard error of the mean (SEM) was determined. The student t-test was used to compare the treated and untreated groups in confocal microscopy. The ordinary one-way ANOVA with Tukey multiple comparisons *posthoc* test was used to determine significant differences among means of each condition against the control in confocal microscopy, western-blot, and flow cytometry assay. For the *in vivo* assays, the Kaplan–Meier survival curves were drawn. The Wilcoxon and Mantel-Cox tests were used to compare the survival rate between treated and untreated groups using the GraphPad Prism 6.0 software. Finally, the ANOVA-LSD test was used to compare the average survival time between treated and untreated groups. In all cases, a $p \leq 0.05$ was considered statistically significant.